

1 **Discovery Reactive chlorine, sulphur and nitrogen containing**  
2 **volatile organic compounds impact atmospheric chemistry in**  
3 **the megacity of Delhi during both clean and extremely polluted**  
4 **seasons of reactive chlorine, sulphur and nitrogen containing**  
5 **ambient volatile organic compounds in the megacity of Delhi**  
6 **during both clean and extremely polluted seasons**

7 Sachin Mishra<sup>1</sup>, Vinayak Sinha<sup>1</sup>, Haseeb Hakkim<sup>1</sup>, Arpit Awasthi<sup>1</sup>, Sachin D. Ghude<sup>2</sup>, Vijay  
8 Kumar Soni<sup>3</sup>, Narendra Nigam<sup>3</sup>, Baerbel Sinha<sup>1</sup>, Madhavan N. Rajeevan<sup>4</sup>

9 <sup>1</sup>Department of Earth and Environmental Sciences, Indian Institute of Science Education and Research Mohali,  
10 Sector 81, S.A.S Nagar, Manauli PO, Punjab, 140306, India

11 <sup>2</sup>Indian Institute of Tropical Meteorology, Pashan, Pune 411 008, Ministry of Earth Sciences, India

12 <sup>3</sup>India Meteorological Department, New Delhi 110 003, India, Ministry of Earth Sciences, India

13 <sup>4</sup>Ministry of Earth Sciences, Government of India, New Delhi 110 003, India

14 \* Correspondence to: Vinayak Sinha ([vsinha@iiser Mohali.ac.in](mailto:vsinha@iiser Mohali.ac.in))

15 **Abstract.** Volatile organic compounds significantly impact the atmospheric chemistry of polluted megacities.  
16 Delhi is a dynamically changing megacity and yet our knowledge of its ambient VOC composition and chemistry  
17 is limited to few studies conducted mainly in winter before 2020 (all pre-~~COVID~~<sup>eovid</sup>). Here, using a new  
18 extended volatility range high mass resolution (10000-15000) Proton Transfer Reaction Time of Flight Mass  
19 Spectrometer<sup>10K</sup>, we measured and analyzed ambient VOC-mass spectra acquired continuously over a four-  
20 month period covering “clean” monsoon (July-September) and “polluted” post-monsoon seasons, for the year  
21 2022. Out of 1126 peaks, 111 VOC species were identified unambiguously. Averaged total mass concentrations  
22 reached ~260 $\mu\text{g m}^{-3}$  and were >4 times in polluted season relative to cleaner season, driven by enhanced emissions  
23 from biomass burning and reduced atmospheric ventilation (~2). Among 111, 56 were oxygenated, 10 contained  
24 nitrogen, 2 chlorine, 1 sulphur and 42 were pure hydrocarbons. VOC levels during polluted periods were  
25 significantly higher than most developed world megacities. Surprisingly, mMethanethiol, dichlorobenzenes, C6-  
26 amides and C9-organic acids/esters, which have previously never been reported in India, were detected in both  
27 the clean and polluted periods. The sources were industrial for methanethiol and dichlorobenzenes, purely  
28 photochemical for the C6-amides and multiphase oxidation and partitioning for C9-organic acids. Aromatic  
29 VOC/CO emission ratio analyses indicated additional biomass combustion/industrial sources in post-monsoon  
30 season, alongwith year-round traffic sources in both seasons. Overall, the unprecedented new information  
31 concerning ambient VOC speciation, abundance, variability and emission characteristics during contrasting  
32 seasons significantly advances current atmospheric composition understanding of highly polluted urban  
33 atmospheric environments like Delhi.

## 35 1 Introduction

36 The national capital territory of Delhi [in India](#) is jointly administered by the central and state governments and  
37 accommodated more than 32 million people in 2022. For the past several years, its population has grown at the  
38 rate of more than 2.7 percent per year, adding about 1 million new inhabitants each year. Thus, the region  
39 represents a complex dynamically changing emission environment driven by rapid changes in emissions as  
40 regulatory authorities make efforts to improve urban infrastructure and public transportation while promoting  
41 cleaner technologies. As a megacity in a developing country with one of the world's highest population densities,  
42 Delhi exemplifies some of the key challenges faced by many megacities in the global south, where increased  
43 urbanization and inequitable access to clean energy sources along with unfavourable meteorological conditions  
44 during cold periods of the year, cause the inhabitants to suffer from extreme air pollution episodes. Lelieveld et  
45 al. (2015) identified South Asia as one of the global air pollution hotspots in terms of the contribution of outdoor  
46 air pollution sources to premature mortality due to particulate matter pollution. Reduction of other atmospheric  
47 pollutants is also deemed necessary to fulfil the UN Sustainable Development Goals (Keywood et al., 2023). Thus,  
48 the study of Delhi's ambient chemical composition using state of the art technology can offer valuable insights  
49 and lessons for our understanding of polluted atmospheric environments.

50 Previous studies have demonstrated that air pollution in the Delhi-NCR metropolitan area peaks during the post-  
51 monsoon (October- November) season (e.g. Kulkarni et al., 2020), coinciding with the time of year when large  
52 scale paddy stubble burning occurs in the Indo-Gangetic Plain (Kumar et al., 2021). The main air pollutant in  
53 exceedance has long been identified to be particulate matter (e.g. PM<sub>2.5</sub>) and many studies (Gani et al., 2020; Cash  
54 et al., 2021; Sharma et al., 2023; Singh et al., 2011) have documented the variability, exceedance and composition  
55 of aerosols. Volatile organic compounds (VOCs) are major precursors of secondary organic aerosol, which is a  
56 significant component of PM<sub>2.5</sub> (30-60% in Delhi; Chen et al., 2022; Nault et al., 2021) and surface ozone over  
57 Delhi. In fact, in-situ ozone production in Delhi has been reported to be more sensitive to VOCs rather than  
58 nitrogen oxides (Nelson et al., 2021). Several VOCs (e.g. benzene, nitromethane, 1,3-butadiene) are also  
59 carcinogenic (WHO 2010) at high exposure concentrations and many pose direct health risks (Ho et al., 2006;  
60 Espenship et al., 2019; WHO 2019; Weng et al., 2009; Roberts et al., 2011; Durmusoglu et al., 2010). VOCs can  
61 also aid source apportionment studies by acting as source fingerprints and valuable molecular markers of specific  
62 emission sources (de Gouw et al., 2017; Holzinger et al., 1999; Warneke et al., 2001; Kumar et al., 2020; Garg et  
63 al., 2016; Hakkim et al; 2021; Kumar et al., 2021). In the complex emission environment of cities in the developing  
64 world, this can be especially helpful since the energy usage portfolio is such that biomass burning sources are  
65 likely to be as significant as fossil-fuel based sources (Bikkina et al., 2019) in influencing the air pollutant burden  
66 of VOCs, resulting in ambient air VOC composition that could be quite different from cities like Los Angeles  
67 (McDonald et al., 2018).

68 Existing knowledge about the abundance and diurnal variability of major ambient VOCs such as methanol,  
69 acetone, acetaldehyde, acetonitrile, isoprene, benzene, toluene, xylenes and trimethyl benzenes in Delhi, is limited  
70 to just four previously measured wintertime datasets: Dec-March of 2016 (Chandra et al., 2018; Hakkim et al.,  
71 2019), Dec-March of 2018 (Wang et al., 2020; Tripathi et al., 2022), few days in October 2018 (Nelson et al.,  
72 2021; Bryant et al., 2023) and one spanning 145 days of 2019 that reported source apportionment of some VOCs  
73 for different seasons (Jain et al., 2022). We note that all these were pre-COVID period datasets, and that since  
74 these observations many new regulations have been put in place e.g. for traffic with the introduction of BS-VI

75 (EURO6 equivalent) in 2020 and the [Faster Adoption and Manufacturing of hybrid and Electric vehicles \(FAME\)](#)  
76 program for promotion of E-vehicles, and for industries with a ban on the use of petcoke in the [National Capital](#)  
77 [Region \(NCR\)](#) and the crackdown on unregistered industries (Guttikunda et al, 2023). [After COVID lock-downs](#)  
78 [happened in 2020, a new Commission for Air Quality Management in –Delhi National Capital Region and its](#)  
79 [Adjoining Areas \(CAQM\) was set up in November 2020 \(https://caqm.nic.in/index.aspx?langid=1 \). Under its](#)  
80 [mandate, depending on air quality level, it promulgates immediate graded response action plans \(GRAP;](#)  
81 [https://caqm.nic.in/index1.aspx?lsid=4168&lev=2&lid=4171&langid=1\)](#) that instruct civic authorities to shut-  
82 [down or restrict particular emission sources. Furthermore, on 7 August 2020, the Delhi government announced a](#)  
83 [new Delhi Electric Vehicle \(EV\) Policy. In order to address the high-upfront cost of EVs \(ICE vehicles\), the Delhi](#)  
84 [EV Policy provides demand incentives for purchasing electric vehicles. The incentives help bring cost parity for](#)  
85 [EVs and are in addition to those outlined in the Faster Adoption and Manufacturing of Hybrid and Electric](#)  
86 [Vehicles \(FAME II\). In the budget allocation for 2020, the Government of India allocated \\$600 million USD for](#)  
87 [clean air measures through the Ministry of Housing and Urban Affairs \(MoHUA\) to 46 cities across India. These](#)  
88 [have been detailed in a report by Arpan Chatterji \(2020\). Thus overall, important changes to the transport emission](#)  
89 [sector, construction and urban industrial sector and residential sector were implemented at a policy level after](#)  
90 [2020 to reduce air pollution in the Delhi-NCR region.](#)

91 The monsoon season which precedes the post-monsoon season lasts from June to September and is characterized  
92 by better air quality, aided by favourable meteorological conditions, including higher ventilation co-efficient,  
93 negligible agricultural waste burning and enhanced wet scavenging (Kumar et al., 2016).

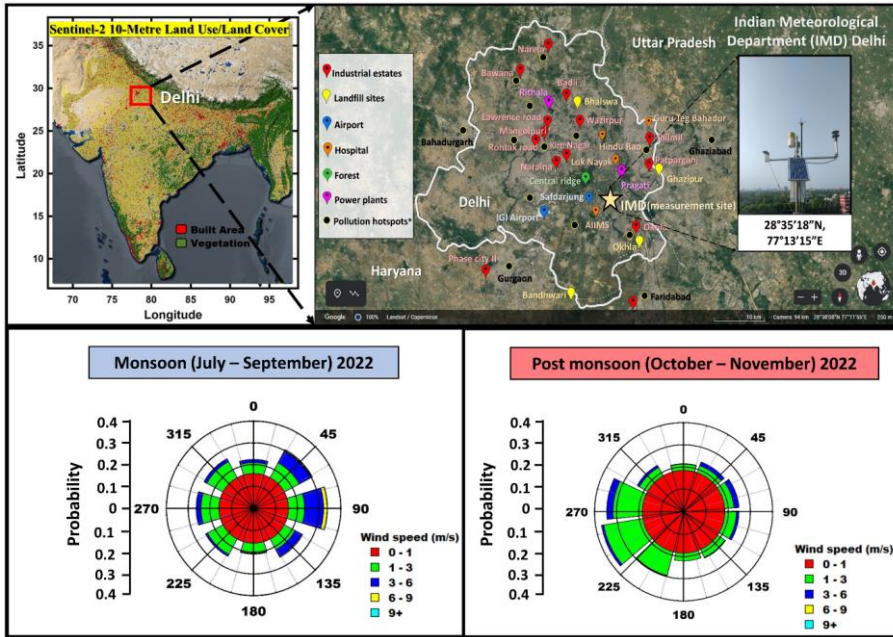
94 This study addresses some of the above knowledge gaps pertaining to ambient VOCs during the “clean” monsoon  
95 season characterized by baseline pollution levels and the polluted “post-monsoon” season characterized by  
96 extreme pollution events and large scale open agricultural biomass waste fires regionally. Employing a new  
97 extended volatility range (EVR) high mass resolution (10000-15000) Proton Transfer Reaction Time of Flight  
98 Mass Spectrometer 10K (PTR-TOF 10000; Ionicon Analytik GmbH), a technology that has never before been  
99 deployed in India, we investigated the ambient VOC speciation, abundance, variability and emission  
100 characteristics in the polluted urban environment of Delhi over a 4-month period. This enabled us to discover  
101 several low volatility VOCs, many of which are present in fire emissions (Koss et al., 2018), for the time in South  
102 Asia, as all previous VOC studies have involved either the older PTR-TOF-MS or PTR-QMS instruments, that  
103 have significantly lower mass resolution and lower detection sensitivity and did not possess the extended volatility  
104 range components. We first undertook comprehensive and rigorous interpretation of the ambient mass spectra  
105 over a four-month period spanning July-Nov of 2022 in Delhi. This was followed by identification and  
106 quantification of 111 VOCs, many of which have been discovered and reported for the first time from the South  
107 Asian atmospheric environment. Each of these compounds was then classified in terms of oxygenated VOCs, pure  
108 hydrocarbons, major nitrogen containing VOCs, chlorine containing VOCs and sulphur containing VOCs,  
109 followed by the time series analyses and diurnal profiles of the major VOCs and some new/rarely reported VOCs  
110 in both seasons as a function of meteorology and emissions. The atmospheric chemistry implications of some of  
111 the newly discovered compounds in this polluted urban environment are discussed. Further, using measured  
112 aromatic VOC/CO emission ratios in monsoon and post-monsoon season, a global comparison with reports from  
113 megacities in Europe, North America and Asia was undertaken for a nuanced understanding of their levels and  
114 sources in Delhi relative to megacities across these different continents.

115 2. Methodology

116 2.1 Measurement site and meteorological conditions:

117

118



119

120 Figure 1: Map of India showing Delhi (1a) and zoom in of the measurement site (star marked) (1b; Google Earth  
121 Imagery © Google Earth) with a view from the roof-top of the SatMet Building (28.5896°N-77.2210°E), and wind rose  
122 plots derived from in-situ one-minute wind speed and wind direction data during monsoon (1c) and post-monsoon  
123 (1d) 2022 acquired at sampling height of ~35m A.G.L.

124

125 The measurement site was located within the premises of the India Meteorological Department (IMD) which is  
126 situated in Central Delhi (Fig. 1). Ambient air was sampled at a height of ~~of eireaof circa~~ circa 35m above ground level  
127 from the roof-top of the SatMet building (28.5896°N-77.2210°E), into the instruments which were housed  
128 inside a laboratory located in the sixth floor of the same building.

129 Figure 1 (a) shows the land use/ land cover (Sentinel-2 10m) map of India with a red marked box highlighting  
130 Delhi. The city is bordered on its northern, western, and southern sides by the state of Haryana and to the east by  
131 the state of Uttar Pradesh. The star marked in Fig. 1 (b) shows the measurement site (IMD Delhi) and its  
132 surroundings. The major pollution hotspots include places like Ghaziabad (towards the northeast), Bahadurgarh  
133 (towards the northwest), Gurgaon (towards the southwest), and Faridabad and Okhla (towards the southeast),  
134 which are highlighted as black dots. Major industrial areas are marked in red (e.g. Okhla industrial area), while  
135 major landfill sites are marked in yellow. The international airport is marked with a blue pointer and some

136 Major hospitals are also marked in orange, forest areas in green, and power plants are marked in sky-blue  
137 colour shown in Fig 1 (b).

138 Meteorological sensors (Campbell Scientific Inc.) were deployed to measure the wind speed, direction,  
139 temperature, relative humidity and photosynthetic active radiation (model nos.: CS215 for temperature and RH,  
140 PAR PQSI sensor, and for rain TE525-L40). Boundary layer height was taken from ERA5 reanalyses dataset  
141 (Hersbach et al., 2023) and ventilation coefficient was calculated as the product of the measured wind speed and  
142 boundary layer height. Atmospheric ventilation or ventilation coefficient (VC) is a good proxy for the dilution  
143 and dispersion of air pollutants near the surface (Hakkim et al., 2019). It is defined as the product of boundary  
144 layer height (m) and wind speed ( $\text{ms}^{-1}$ ). The VC represents the rate at which air within the mixed layer is  
145 transported away from a region of interest and provides information about how concentrations of pollutants are  
146 modulated through transport of air over that region. Figures 1 (c) and 1 (d) show the wind rose plot derived from  
147 the in-situ one-minute wind speed and wind direction data acquired at the measurement site for monsoon (July  
148 2022 – September 2022) and post-monsoon (October 2022 – November 2022) seasons, respectively. The prevalent  
149 wind direction changed from easterly flow in monsoon season to westerly flow in the post-monsoon season.  
150 During the monsoon season, the major fetch region spanned from the NE to SE-E. These NE, E, and SE winds  
151 were associated with high wind speeds ranging from 3 – 6  $\text{ms}^{-1}$ , which on occasions reached up to 9  $\text{ms}^{-1}$ . During  
152 the post-monsoon season, the major wind flow was from the NW to the SW-W sector. These wind speeds were  
153 lower, ranging from 1 – 3  $\text{ms}^{-1}$  exceeding 6  $\text{ms}^{-1}$  only occasionally. Overall, the site received air from all wind  
154 sectors in both seasons. This is also borne by the back trajectory analyses presented in the companion paper  
155 (Awasthi et al., 2024), which showed that the site is characterized by regional airflow patterns as documented at  
156 other sites in the Indo-Gangetic Plain (Pawar et al., 2015).

157 Fire count data were obtained using the Visible Infrared Imaging Radiometer Suite (VIIRS) 375m thermal  
158 anomalies/active fire product data from the VIIRS sensor aboard the joint NASA/NOAA Suomi National Polar-  
159 orbiting Partnership (Suomi NPP) and NOAA-20 satellites for high and normal confidence intervals only.

## 160 2.2 Measurement of Volatile Organic Compounds using the PTR-TOF-MS 10K

161 Volatile organic compounds (VOCs) were measured using a new high sensitivity and high mass resolution Proton  
162 Transfer Reaction Time of Flight Mass Spectrometer (PTR-TOF-MS 10k, model PT10-004 manufactured by  
163 Ionicon Analytik GmbH, Austria). While PTR-TOF-MS 8000 series (Tripathi et al., 2022) and PTR-QMS (Sinha  
164 et al., 2014) instruments have been previously deployed in India and have mass resolutions of 8000 and 1,  
165 respectively, this study marks the first deployment of the PTR-TOF-MS 10K system in India, a system that  
166 possesses several unique advantages over the older generation instruments for VOC measurements in polluted  
167 and complex emission environments. The first is that this new system is equipped with the extended volatility  
168 range technology (Piel et al., 2021), ensuring that even many intermediate volatility range compounds and sticky  
169 VOCs can be detected with very fast response times and minimal surface effects. The inlet system of the  
170 instrument as well as the ionization chamber is fully built into a heated chamber and the inlet capillary is further  
171 fed through a heated hose to ensure there are no “cold” spots for condensation. The entire inlet system is made of  
172 inert material (e.g. PEEK or siliconert treated steel capillaries to keep surface effects minimal. Additionally, a 7  
173  $\mu\text{m}$  siliconert filter just before the drift tube served to minimize clogging/contamination of the system. The second  
174 advantage possessed by the PTR-TOF-10K used in this work is the inclusion of an ion booster funnel and hexapole

Formatted: Superscript

175 ion guide placed after the drift tube/reaction chamber for improved extraction of ions in a manner that boosts both  
176 the mass resolution as well as the sensitivity over its older peers. This helped achieve much higher mass resolution  
177 (> 10000 m/Δm), even reaching as high as 15000 m/Δm at m/z 330, and detection limits better than 3 ppt for all  
178 compounds detected in the mass to charge ratio (m/z) 31-330 mass range. These customizations over previously  
179 deployed PTR-TOF-MS instruments in Delhi, enabled detection and discovery of several intermediate range-  
180 volatility compounds (IVOCs) in the gas phase. Other parts of the instrument ~~consisted of proven PTR-TOF-MS~~  
181 ~~technology in the form of a hollow cathode ion source, which produces a stream of pure H<sub>2</sub>O<sup>+</sup> through the plasma~~  
182 ~~discharge of water vapour, the reaction chamber/drift tube where the VOCs (Analyte molecules) having proton~~  
183 ~~affinity higher than that of H<sub>2</sub>O (164.8 kcal mol<sup>-1</sup>) underwent primarily soft chemical ionization typically forming~~  
184 ~~the corresponding protonated molecular ions. At the end of the lens system, the ions entered the pulser region~~  
185 ~~through an aperture and were accelerated in the TOF region (Time of Flight), a field-free region where the ions~~  
186 ~~rebounded in a reflectron and were refocused and detected using a Multi-Channel Plate (MCP) detector (Burle~~  
187 ~~Industries Inc., Lancaster, PA, USA.). These aspects of the PTR-TOF-MS technology have already been explained~~  
188 well earlier (Jordan et al., 2009; Graus et al., 2010). During this study, the instrument was operated at a drift tube  
189 pressure of 3 mbar, drift tube temperature of 120 °C, and drift tube voltage of 600V, resulting in an operating E/N  
190 ratio of ~ 120 Td (1 Td = 10<sup>-17</sup> V cm<sup>-2</sup>). These operational instrumental settings are also summarized in Table S1.  
191 Ambient air was sampled continuously from the rooftop (~35m A.G.L) through a Teflon inlet line that was  
192 protected with a Teflon membrane particle filter (0.2 μm pore size, 47 mm diameter) to ensure that dust and debris  
193 did not enter the sampling inlet. ~~The length of the inlet line was 5m and made of Teflon (3m 1/8 inch O.D. and~~  
194 ~~2m 1/4inch O.D). The total inlet residence time was ~2.7 seconds. The part of the inlet that was indoors (3m of~~  
195 ~~1/8 inch O.D.) was well insulated and heated to 80 degree Celsius. We think this short inlet residence time and~~  
196 ~~heated inlet facilitated the detection of IVOCs, relative to previous studies. The part of the inlet line that was~~  
197 ~~indoors was well insulated inside a black hose and heated to 80 °C.~~The instrument background was acquired  
198 regularly (typically every 30 min for 5 min), by sampling VOC-free zero air. VOC-free zero air was produced by  
199 passing air through an activated charcoal scrubber (Supelpure HC, Supelco, Bellefonte, USA) and a VOC  
200 scrubber catalyst (Platinum wool) maintained at 370 °C. Mass spectra covering the m/z 15 to m/z 450 range were  
201 obtained at 1 Hz frequency. An internal standard comprising 1,3-di-iodobenzene (C<sub>6</sub>H<sub>3</sub>I<sub>2</sub><sup>+</sup>) detected at m/z 330.848  
202 and its fragment ion [C<sub>6</sub>H<sub>3</sub>I<sup>+</sup>] detected at m/z 204.943 were constantly injected to ensure accurate mass axis  
203 calibration, so that any drifts in the mass scale were corrected providing for accurate peak detection. Primary data  
204 acquisition of mass spectra was accomplished using the ionTOF software (version 4.2; IONICON Analytik  
205 Ges.m.b.H., 6020 Innsbruck, Austria). ~~This software allows the user to define and perform measurements and~~  
206 ~~displays the measured data in real-time.~~All the settings related to PTR (Proton Transfer Reaction), TPS (TOF  
207 power supply), MPV (Multi-port-valve), and MCP (Multi-channel plate) can be controlled and optimized using  
208 this control software. The raw mass spectra and relevant instrumental metadata are stored in HDF5 format. These  
209 spectra were further processed using the Ionicon Data Analytik (IDA version 2.2.0.4; Ionicon Analytik GmbH,  
210 Innsbruck, Austria) software that has the functionalities for peak search, peak fits and preliminary mass  
211 assignments and identification of a broad spectrum of organic compounds. The IDA software employs an  
212 automated peak detection routine guided by user-defined sensitivity levels for peak detection, peak fit, and shape.  
213 The software then uses chemical composition information based on the exact masses and isotopic patterns and  
214 calculates a specific proton transfer rate constant (k-rate) based on the polarizability and dipole moment for the

215 peaks with an assigned chemical formula, instead of using a generic value as was done in previous PTR-TOF-MS  
216 measurements in Delhi (Tripathi et al., 2022). We manually ~~checked~~-compared the values also with the  
217 compilation of k rates reported by Pagonis et al., (2019) as an additional check. The user has possibility to define  
218 a window for mass accuracy (e.g. 30 ppm). Within this defined range and accuracy window, the software identifies  
219 all possible chemical compositions and molecular formulae and calculates the corresponding isotope patterns.  
220 These patterns are then compared to find the best-fit chemical composition. The process is carried out iteratively,  
221 starting with the lower m/z values, according to the method described in the study by Stark et al., (2015).  
222 In this study, a total of 1126 peaks were detected in the raw measured ambient mass spectra. After further  
223 additional quality control and assurance steps performed manually as detailed in the Section 3.0, 111 compounds  
224 present in ambient air for which the molecular formula could be confirmed unambiguously are reported and for  
225 which isotopologues due to molecules of different chemical composition could be ruled out completely, were  
226 further analysed in this work. The term “unambiguous” is used in the context of the accurate elemental  
227 composition/molecular formula assignment of the ions by leveraging the high mass resolution (8000-13000 over  
228 entire dynamic mass range) and detection sensitivity (reaching even 1 ppt or better for many ions; see Table S2)  
229 of the instrument. This enabled ensuring peaks due to expected isotopic signals were not construed as new  
230 compounds if their height was exactly as expected for a shoulder isotopic peak based on the natural abundance of  
231 isotopes of carbon, hydrogen, nitrogen, sulphur, chlorine and oxygen that made up the more abundant molecular  
232 ion. Where an ion could occur significantly due to fragmentation of another compound, the same has also been  
233 noted in Table S2 during attribution of the compound’s name. -Figure S1 -provides an example of visualization of  
234 mass spectra and peak assignment using the IDA software which also illustrate the high mass resolving power of  
235 the PTR-ToF-MS 10K, that enables separation of ion signals that differ by less than 0.04 Th, as well the  
236 identification of isotopic peaks of parent compounds like methanethiol, dichlorobenzene, C-6 amide and C-9  
237 carboxylic acid acid (Fig S2), which are discussed in detail in Section 2.4. Table S2 also provides the limit of  
238 detection (LoD) of the compounds as well as the average and interquartile range observed season-wise for each  
239 ion. The LoD was calculated by taking the 2 $\sigma$  value of the VOC-free zero air instrument background (Müller et  
240 al., 2014). Example of measured data showing the instrumental backgrounds and ambient levels for methanethiol,  
241 dichlorobenzene, C-6 amide and C-9 carboxylic acid acid, over a 3h period are illustrated in Fig S3. A certified  
242 VOC calibration gas mixture (Societa Italiana Acetilene E Derviat; S.I.A.D. S.p.A., Italy) containing 11  
243 hydrocarbons at ~100 ppb, namely methanol, acetonitrile, acetone, isoprene, benzene, toluene, xylene,  
244 trimethylbenzene, and dichlorobenzene and trichlorobenzene was used during the field deployment for measuring  
245 the transmission and sensitivity of compounds covering the mass range (m/z=33 to m/z = 181). The instrument  
246 was calibrated a total of 8 times during the study period: 21.07.2022 after first installation, 26.09.2022,  
247 21.10.2022, 26.10.2022, 5.11.2022, 11.11.2022, 16.11.2022 and 30.11.2022. Results were reproducible (~21% or  
248 better for all compounds) across all experiments and a transmission curve obtained from one of the calibration  
249 experiments is shown in Fig. S42. Measured transmission further allowed for more accurate quantification by  
250 accounting for correction of the mass-dependent detection efficiency of the system. Equation S1 (de Gouw et al.,  
251 2007) was then used to convert the measured ion signals to mixing ratios. The linearity for compounds available  
252 in the VOC standard were also checked independently and was above  $r \geq 0.9$  as illustrated in Fig S53 for the tested  
253 range of ~2 to 8 ppb. The background corrected concentrations of all the detected m/z were exported from IDA in  
254 .csv format and further analysis of the dataset was carried out using IGOR Pro software (version 6.37;

WaveMetrics, Inc.). [The overall uncertainty calculated using the root mean square propagation of errors due to the accuracy of gas standard and flow controllers was ~13 % or better for compounds present in the VOC gas standard. For other compounds reported in this work, it is estimated that the combined accuracy of the transmission function and the parameterized k-rates, put the overall uncertainty in the range of ±30% \(Reinecke et al., 2024\).](#)

Carbon monoxide (CO) was measured using IR filter correlation-based spectroscopy air quality analyzer (Thermo Fischer Scientific 48i) while ozone was measured using UV absorption photometry (Model 49i; Thermo Fischer Scientific, Franklin, USA). The overall uncertainty of the measurements was less than 6%. Details concerning characterization of the instrument including calibration and data QA/QC protocols have been comprehensively described in our previous works (Chandra and Sinha, 2016; Kumar et al., 2016; Sinha et al., 2014).

### [2.3 Mass assignment and compound identification](#)

[A total of 1126 peaks were detected in the raw mass spectra. To identify the ambient compounds of relevance in Delhi from these detected peaks, the following additional manual quality control checks were undertaken. First, peaks attributed to non-ambient compounds such as the impurity ions \(e.g. NO<sup>+</sup>\), water cluster ion peaks, and peaks associated with internal standards were excluded resulting in 1025 peaks for further consideration. Next, the diel profiles and detection limits of these 1025 ion peaks were perused. Only 319 ions out of the 1025 ions showed some diurnal variability and had values above the detection limit after accounting for the respective instrumental background. Next, we verified the presence and expected theoretical magnitude of the shoulder isotopic peaks based on the natural isotopic distribution abundance of the elemental composition of the ion. Fig S6 provides a visual example. This was feasible for all m/z except the C1 oxygen containing analyte ions, where the shoulder peak was below detection limit. The preceding QA/QC resulted in an unambiguous assignment for 111 of the 319 ions. Note that these 111 explained 86% of the total mass concentration \( \$\mu\text{g m}^{-3}\$ \) observed due to the 319 detected peaks when accounting for the isotopic peaks as well. Table S2 lists the ion m/z and molecular formula of the corresponding compound, along with the averaged mixing ratios observed in each case during the monsoon and post-monsoon season. Additionally, the characteristic ambient diel profile classification as one of the following: unimodal with daytime peak for biogenic/ evaporative/ photochemical source emitted compounds, bimodal with morning and evening peaks for compounds driven by primary emissions \(e.g. toluene\) and trimodal which were hybrid of the former two, are also provided for each species. Compound names were attributed to specific ions using assignments reported at that m/z in the compiled peer-reviewed PTR-MS mass libraries published by Yáñez-Serrano et al., \(2021\) and Pagonis et. al., \(2019\) as well as previously published pioneering reports by Stockwell et. al. \(2015\), Sarkar et al. \(2016\), Yuan et al. \(2017\) and Hatch et al. \(2017\).](#)

[Fragmentation of certain compounds in specific atmospheric environments can cause significant interferences in the detection of major compounds like isoprene, acetaldehyde and benzene, as reported recently by Coggon et al., 2024. We checked these as well as an additional quality control measure. As noted by Coggon et al. 2024, isoprene can suffer significant interferences from higher aldehydes as well as substituted cyclohexanes, which can fragment and add to the signal at m/z 69.067 \(at which protonated isoprene C<sub>5</sub>H<sub>9</sub><sup>+</sup> is also detected\). The magnitude depends on the instrument operating conditions \(Townsend ratio\), instrument design and the mixture of VOCs present in ambient air while co-sampling isoprene. Coggon et al. 2024 very nicely clarified both these aspects and found that when influenced by cooking emissions and oil and natural gas emissions and at higher Townsend ratios, these](#)

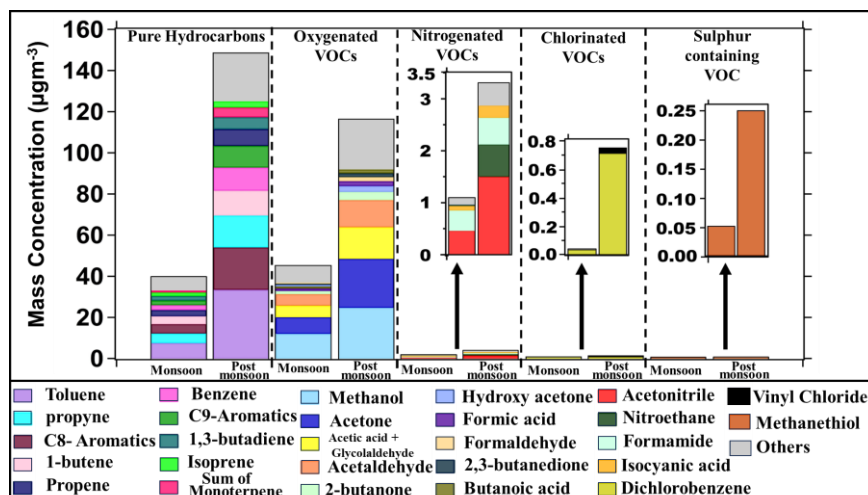


294 [interferences can be quite significant and even account for upto 50% of the measured signal attributed to isoprene](#)  
295 [in extreme cases. We operated the PTR-TOF-MS at 120 Td which minimizes fragmentation even if it occurs,](#)  
296 [compared to when operated at 135-140 Td. Concerning the ambient VOC mixture and emission sources, we note](#)  
297 [that the type of restaurant cooking emissions present in Las Vegas and over Oil and Natural Gas petrochemical](#)  
298 [facilities in USA for which Coggon et al. 2024 reported the highest isoprene interferences, were absent/negligible](#)  
299 [at the study site in Delhi. In the latter, open biomass burning sources such as paddy residue burning in post-](#)  
300 [monsoon season and garbage biomass fires and traffic that occur throughout the year are ~~significantly~~ more](#)  
301 [significant~~important~~.](#) Use of more specific though slower analytical techniques based on gas chromatography  
302 [show that such biomass combustion sources ~~are known to~~ emit significant amounts of isoprene \(Andrea et al.,](#)  
303 [2019; Kumar et al., 2021\). The above points and supporting TD-GC-FID measurements of isoprene, benzene and](#)  
304 [toluene \(see Fig S7 and ~~Shabin et al., 2024~~\), led us to conclude that such correction is unwarranted for our PTR-](#)  
305 [TOF-MS dataset. Concerning the interference on acetaldehyde detection due to ethanol, we note that even in](#)  
306 [Coggon et al. 2024 this was reported to only be of significance in highly concentrated ethanol plumes such as](#)  
307 [those encountered on the Las-Vegas strip where ~1500 ppb of ethanol was detected. On the contrary, in Delhi as](#)  
308 [listed in Table S2, ethanol values detected at m/z 47.076 were on average only 0.2 ppb \(Interquartile range 0.16](#)  
309 [ppb\) during monsoon and 0.55 ppb \(Interquartile range 0.5 ppb\) in post-monsoon season, respectively, whereas](#)  
310 [acetaldehyde detected at m/z 45.03 was significantly higher at 3.34 and 7.75 ppb during monsoon and post-](#)  
311 [monsoon season, respectively.](#)  
312 [For the same molecular formula, several isomeric compounds with differing chemical structures are possible, with](#)  
313 [the number of possibilities increasing enormously with an increase in the number of atoms that make up the](#)  
314 [molecule. In addition, in some instances fragmentation of other compounds can complicate the compound](#)  
315 [attribution for a given ion. Nonetheless in the interest of stimulating interest and further investigation as many](#)  
316 [have been previously rarely reported or are being reported for the first time in ambient air, we have made bold to](#)  
317 [provide one of the many possible chemical structures in the Table S2. We do caution that the chemical structure](#)  
318 [provided by no means even constitutes a best guess estimate but nonetheless would be appealing to chemists and](#)  
319 [provoke further detailed reporting rather than just the molecular formula.](#)

### 321 **3. Result and Discussion:**

#### 322 **3.1: Analyses of ambient mass spectra and mass concentration contributions of VOC chemical classes**

323



324  
 325 **Figure 2: Bar graph** Histogram of 111 compounds class-wise, namely Pure Hydrocarbons, Oxygenated VOCs  
 326 (OVOCs), Nitrogen-containing VOCs (NVOCs), Chlorine-containing VOCs (ClVOCs), and sulphur-containing VOC  
 327 (SVOC) in both monsoon and post-monsoon periods.

328  
 329 A total of 1126 peaks were detected in the raw mass spectra. To identify the ambient compounds of relevance in  
 330 Delhi from these detected peaks, the following additional manual quality control checks were undertaken. First,  
 331 peaks attributed to non-ambient compounds such as the impurity ions (e.g. NO<sup>+</sup>), water cluster ion peaks, and  
 332 peaks associated with internal standards were excluded resulting in 1025 peaks for further consideration. Next,  
 333 the diel profiles and detection limits of these 1025 ion peaks were perused. Only 319 ions out of the 1025 ions  
 334 showed some diurnal variability and had values above the detection limit after accounting for the respective  
 335 instrumental background. Next, we verified the presence and expected theoretical magnitude of the shoulder  
 336 isotopic peaks based on the natural isotopic distribution abundance of the elemental composition of the ion. Fig S  
 337 provides a visual example. This was feasible for all m/z except the C1 oxygen-containing analyte ions, where the  
 338 shoulder peak was below detection limit. The preceding QA/QC resulted in an unambiguous assignment for 111  
 339 of the 319 ions. Note that these 111 explained 86% of the total mass concentration (µgm<sup>-3</sup>) observed due to the  
 340 319 detected peaks when accounting for the isotopic peaks as well. Table S2 lists the ion m/z and molecular  
 341 formula of the corresponding compound, along with the averaged mixing ratios observed in each case during the  
 342 monsoon and post-monsoon season. Additionally, the characteristic ambient diel profile classification as one of  
 343 the following: unimodal with daytime peak for biogenic/evaporative/photochemical source emitted compounds,  
 344 bimodal with morning and evening peaks for compounds driven by primary emissions (e.g. toluene) and trimodal  
 345 which were hybrid of the former two, are also provided for each species. Compound names were attributed to  
 346 specific ions using assignments reported at that m/z in the compiled peer-reviewed PTR-MS mass libraries  
 347 published by Yáñez-Serrano et al., (2021) and Pagonis et al., (2019) as well as previously published pioneering  
 348 reports by Stockwell et al. (2015), Sarkar et al. (2016), Yuan et al. (2017) and Hatch et al. (2017).  
 349 Fragmentation of certain compounds in specific atmospheric environments can cause significant interferences in  
 350 the detection of major compounds like isoprene, acetaldehyde and benzene, as reported recently by Coggon et al.

351 [2024](#). We checked these as well as an additional quality control measure. As noted by [Coggon et al. 2024](#), isoprene  
352 can suffer significant interferences from higher aldehydes as well as substituted cyclohexanes, which can fragment  
353 and add to the signal at  $m/z$  69.067 (at which protonated isoprene  $C_8H_9^+$  is also detected). The magnitude depends  
354 on the instrument operating conditions (Townsend ratio), instrument design and the mixture of VOCs present in  
355 ambient air while co-sampling isoprene. [Coggon et al. 2024](#) very nicely clarified both these aspects and found that  
356 when influenced by cooking emissions and oil and natural gas emissions and at higher Townsend ratios, these  
357 interferences can be quite significant and even account for upto 50% of the measured signal attributed to isoprene  
358 in extreme cases. We operated the PTR-TOF-MS at 120 Td which minimizes fragmentation even if it occurs,  
359 compared to when operated at 135-140 Td. Concerning the ambient VOC mixture and emission sources, we note  
360 that the type of restaurant cooking emissions present in Las Vegas and over Oil and Natural Gas petrochemical  
361 facilities in USA for which [Coggon et al. 2024](#) reported the highest isoprene interferences, were absent/negligible  
362 at the study site in Delhi. In the latter, open biomass burning sources such as paddy residue burning in post-  
363 monsoon season and garbage biomass fires and traffic that occur throughout the year are significantly more  
364 important. Use of more specific though slower analytical techniques based on gas chromatography show that such  
365 biomass combustion sources are known to emit significant amounts of isoprene ([Andrea et al., 2019](#); [Kumar et  
366 al., 2021](#)). The above points and supporting TD-GC-FID measurements of isoprene, benzene and toluene (Fig S)  
367 (data: [Shabin et al., 2024](#)), led us to conclude that such correction is unwarranted for our PTR-TOF-MS dataset.  
368 Concerning the interference on acetaldehyde detection due to ethanol, we note that even in [Coggon et al. 2024](#)  
369 this was reported to only be of significance in highly concentrated ethanol plumes such as those encountered on  
370 the Las Vegas strip where ~1500 ppb of ethanol was detected. On the contrary, in Delhi as listed in Table S2,  
371 ethanol values detected at  $m/z$  47.076 were on average only 0.2 ppb (Interquartile range 0.16 ppb) during monsoon  
372 and 0.55 ppb (Interquartile range 0.5 ppb) in post monsoon season, respectively whereas acetaldehyde detected  
373 at  $m/z$  45.03 was significantly higher at 3.34 and 7.75 ppb during monsoon and post monsoon season, respectively.  
374 For the same molecular formula, several isomeric compounds with differing chemical structures are possible,  
375 with the number of possibilities increasing enormously with an increase in the number of atoms that make up the  
376 molecule. In addition, in some instances fragmentation of other compounds can complicate the compound  
377 attribution for a given ion. Nonetheless in the interest of stimulating interest and further investigation as many  
378 have been previously rarely reported or are being reported for the first time in ambient air, we have made bold to  
379 provide one of the many possible chemical structures in the Table S2. We do caution that the chemical structure  
380 provided by no means even constitutes a best guess estimate but nonetheless would be appealing to chemists and  
381 provoke further detailed reporting rather than just the molecular formula.

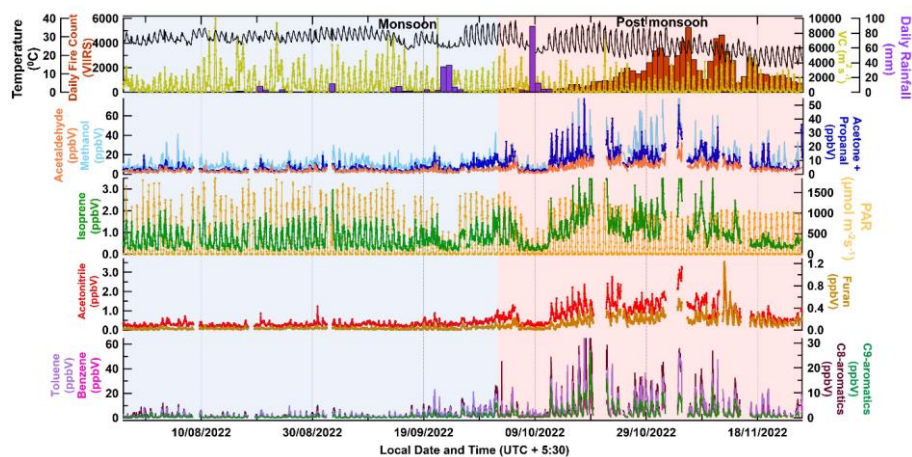
382 A summary of the distribution of the 111 compounds in terms of chemical classes showing their averaged  
383 measured ambient mass concentration ( $\mu\text{g m}^{-3}$ ) contributions is shown in Fig. 2 for the monsoon (22<sup>nd</sup> July – 30<sup>th</sup>  
384 September 2022) and post-monsoon seasons (1 October- 26 November 2022). Out of the 111 compounds, 42 were  
385 pure hydrocarbons made up only of carbon and hydrogen atoms, 56 were oxygenated volatile organic compounds  
386 (OVOCs) made up of only carbon, hydrogen and oxygen, 10 contained nitrogen (NVOCs), 2 contained chlorine  
387 (ClVOCs), and 1 contained sulphur (SVOC). The average total mass concentration of the same set of pure  
388 hydrocarbons during post-monsoon season was 3.7 times greater than in monsoon season ( $40 \mu\text{g m}^{-3}$  vs  $148 \mu\text{g m}^{-3}$ )  
389 while the average total mass concentration of OVOCs during post-monsoon was 2.6 times greater than the  
390 monsoon season values ( $44 \mu\text{g m}^{-3}$  vs  $116 \mu\text{g m}^{-3}$ ). Pure hydrocarbons and OVOCs contributed similarly to the

391 mass concentrations in monsoon season but during the post-monsoon season, the contribution of pure  
392 hydrocarbons was significantly higher than that of OVOCs, due to an increase in primary emissions of these  
393 compounds. The average mass concentration of NVOCs during post-monsoon was thrice as high relative to the  
394 monsoon season ( $1 \mu\text{gm}^{-3}$  and  $3 \mu\text{gm}^{-3}$ ). For the chlorine containing VOCs the post-monsoon, concentrations were  
395 20 times higher, though in absolute magnitude, the values were low ( $1 \mu\text{gm}^{-3}$ ). The average mass concentration of  
396 sulphur containing VOCs during post-monsoon was 4 times higher, but again absolute values were low ( $0.2 \mu\text{gm}^{-3}$ ).  
397 The top 10 pure hydrocarbon compounds by mass concentration ranking were toluene, sum of C8-aromatics  
398 (xylene and ethylbenzene isomers), propyne, 1-butene, benzene, sum of C9-aromatics (trimethyl benzene  
399 isomers), propene, sum of monoterpenes, isoprene and 1,3 butadiene and contributed to 84% of the total mass  
400 concentration due to pure hydrocarbons during both the monsoon and post-monsoon seasons, respectively, while  
401 the top 20 contributed to 95% and 96% of the total mass concentration in monsoon and post-monsoon,  
402 respectively. The top 10 OVOCs: methanol, acetone, acetic acid+ glycolaldehyde, acetaldehyde, hydroxyl-  
403 acetone, formaldehyde, 2-butanone, 2,3-butanedione, formic acid, butanoic acid collectively contributed to 84%  
404 and 79% of the total mass concentration due to all OVOCs in monsoon and post-monsoon, respectively, while the  
405 top 20 contributed to 93% and 90% of the total mass concentration in monsoon and post-monsoon, respectively.  
406 The top 4 NVOCs namely acetonitrile, nitroethane, formamide and isocyanic acid contributed to 92% and 91%  
407 of the total mass concentration in monsoon and post-monsoon, respectively. Out of 2 identified chlorine containing  
408 VOCs, dichlorobenzene ( $\text{C}_6\text{H}_4\text{Cl}_2$ ) was found to be the major contributor contributing 87% and 95% of the total  
409 mass concentration in monsoon and post-monsoon, respectively. The only sulphur containing VOC was  
410 methanethiol [ $\text{CH}_4\text{S}$ ] detected at its protonated ion  $m/z$  49.007 and confirmed by the shoulder isotopic peak.  
411 Overall, there was an increase in the mass concentration of all the classes of VOCs from monsoon to post-  
412 monsoon. This increase in mass concentration could be attributed to increased emissions from sources that get  
413 active in post-monsoon, such as regional post-harvest paddy residue burning, increased open waste burning as  
414 well reduced wet scavenging and ventilation coefficient compared to the monsoon season. We examine these in  
415 more detail in the next sections.

### 416 3.2: Time series of VOC tracers during the “clean” monsoon and “polluted post-monsoon” seasons in Delhi

417

418



419

420

421 **Figure 3: Time series of hourly data for meteorological parameters like temperature (C) and ventilation coefficient**  
 422 **( $\text{m}^2\text{s}^{-1}$ ), daily rainfall and daily fire counts (top panel); hourly mixing ratios of methanol, acetaldehyde, and the sum of**  
 423 **acetone and propanol (second panel from top); isoprene and PAR ( $\mu\text{mol m}^{-2}\text{s}^{-1}$ ) (third panel); acetonitrile and furan**  
 424 **(second panel from bottom); and benzene, toluene and the sum of C8 – aromatics (xylene and ethylbenzene isomers)**  
 425 **and the sum of C9 – aromatics (isomers of trimethyl benzene and propyl benzene) (bottom panel). The blue and red**  
 426 **shaded regions represent the monsoon and post-monsoon periods, respectively.**

427

428 Figure 3 shows the time series plot of meteorological parameters and the mixing ratios of some key VOC tracer  
 429 molecules during monsoon (22<sup>nd</sup> July – 30<sup>th</sup> September 2022, blue-shaded region) and post-monsoon (1<sup>st</sup> October  
 430 – 26<sup>th</sup> November 2022, red-shaded region). The top panel shows the ambient Temperature ( $^{\circ}\text{C}$ ), daily VIIRS fire  
 431 counts on the left side of the top panel and ventilation coefficient ( $\text{m}^2\text{s}^{-1}$ ), and daily rainfall (mm) on the right side  
 432 of the top panel during the study period (22<sup>nd</sup> July 2022 – 26<sup>th</sup> November 2022). A grid ( $1\text{km} \times 1\text{km}$ ) with latitudes  
 433 between  $21^{\circ}\text{N}$  and  $32^{\circ}\text{N}$  and longitudes between  $78^{\circ}\text{E}$  and  $88^{\circ}\text{E}$  was considered for extracting the fire count data.  
 434 The second panel from the top represents the time series of mixing ratios of OVOCs which can be formed photo-  
 435 chemically as well as be emitted from anthropogenic sources, namely methanol, acetaldehyde, and the sum of  
 436 acetone and propanol; the third panel shows the mixing ratio of isoprene (a daytime biogenic chemical tracer, pure  
 437 hydrocarbon) and photosynthetic active radiation (PAR) ( $\mu\text{mol photons m}^{-2} \text{s}^{-1}$ ), and the fourth panel shows the  
 438 mixing ratio of acetonitrile (a biomass burning chemical tracer) and furan (a combustion chemical tracer). The  
 439 bottom panel shows the mixing ratios of benzene, toluene, the sum of C8–aromatics (xylene and ethylbenzene  
 440 isomers), and the sum of C9–aromatics (trimethylbenzene and propyl benzene isomers). These are some of the  
 441 most abundant VOCs typically present in any urban megacity environment, due to their strong emission from  
 442 traffic and industries in addition to biomass burning (Sarkar et al., 2016; Sinha et al., 2014; Chandra et al., 2016;  
 443 Singh et al., 2023; Dolgorouky et al., 2012; Yoshino et al; 2012; Langford et al., 2010). We note that all the  
 444 meteorological conditions and fire activity and VOC levels changed significantly between the much “cleaner”  
 445 monsoon season and “highly polluted” post-monsoon season at the same site. While the average temperature  
 446 during monsoon season was  $29.5 \pm 2.8$   $^{\circ}\text{C}$ , in the post-monsoon season this changed to  $24.8 \pm 5.2$   $^{\circ}\text{C}$ , while the  
 447 average ventilation co-efficient was 1.7 times higher during monsoon season relative to the post-monsoon season.

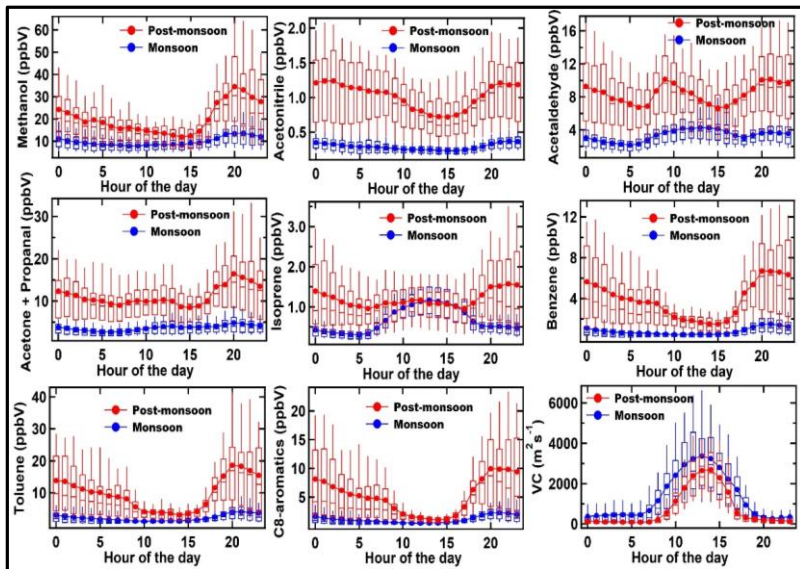
448 Except for the period impacted by heavy rainfall due to western disturbance weather (8th Oct – 10th Oct 2022),  
449 the average mixing ratios for all compounds were considerably higher in the post-monsoon season relative to the  
450 monsoon season even after accounting for the ventilation coefficient reduction with all the aromatics compounds  
451 like benzene, toluene, sum of C8 and C9 aromatics, all 4.5 times higher and furan more than 5 times higher and  
452 acetonitrile, acetone more than 3 times higher and methanol and acetaldehyde 2 times higher. Even isoprene was  
453 1.7 times higher but its night time mixing ratios were higher than daytime mixing ratios during post-monsoon  
454 season relative to the monsoon season. The increases clearly exceed what can be accounted for only by the reduced  
455 ventilation co-efficient (seasonality) and suggests an increase in anthropogenic combustion related sources in  
456 particular from open biomass burning fire sources, which we investigate in more detail in the subsequent sections.

### 457 3.3: Analyses of the diel profiles during the “clean” monsoon and “polluted post-monsoon” seasons in Delhi 458 for discerning major drivers of their ambient values

459 Figure 4 shows the diel box and whiskers plot depicting the average, median, and variability (10th, 25th, 75th and  
460 90th percentile) of the same key VOCs like methanol, acetonitrile, acetaldehyde, acetone and propanal, furan,  
461 isoprene, benzene, toluene and C8 - aromatics for monsoon (derived from ~ 1704 data points, blue markers) and  
462 post-monsoon (derived from ~1368 data points, red markers) against the hour of the day (the horizontal axis  
463 represents the start time of the corresponding hourly bin). This more clearly brings out the season-wise diel  
464 variation of the compounds and in turn throws light on the emission characteristics and how they vary for the  
465 same compound between seasons. Both in the monsoon and post-monsoon season, methanol mixing ratios seem  
466 to be driven by primary emission sources and correlate very well with toluene, a tracer for traffic emissions, with  
467 highest increases in the evening hours (17:00 to 20:00 L.T.). Globally the main source of methanol is vegetation  
468 but in a megacity like Delhi that possesses more than 150000 compressed natural gas (CNG) vehicles and light  
469 duty diesel vehicles, it appears that traffic (see Fig 1 of (Hakkim et al., 2021) emitted methanol controls its ambient  
470 abundance. Similarly, based on the correlation with toluene, traffic emissions seem to be a major contributor for  
471 acetaldehyde, acetone, sum of C8-aromatics and benzene in the morning and evening hours. All these compounds  
472 are among the most abundant VOCs detected in tailpipe exhaust samples (Hakkim et al., 2021). Average ambient  
473 mixing ratios of acetonitrile, a compound emitted significantly from biomass burning (Holzinger et al., 1999),  
474 were below 0.5 ppb in the monsoon for all hours, with only slight increase at night, but during post-monsoon  
475 season, for all hours the values doubled to 1 ppb, with strong increases in the early evening and night time hours.  
476 This tendency was mirrored in all the other compounds including isoprene. The diel profile of isoprene and  
477 acetaldehyde were the only ones which showed daytime maxima during the monsoon season.

478 This shows that during the monsoon season, the biogenic sources of isoprene majorly drive its ambient mixing  
479 ratios, whereas acetaldehyde ambient mixing ratios are controlled by photochemical production of the compound  
480 in the monsoon season. Under the high NOx conditions prevalent in a megacity like Delhi, photo-oxidation of n-  
481 butane, propene, ethane and propane could be a large photochemical source of acetaldehyde (Millet et al., 2010).  
482

Formatted: Font: 10 pt, Font color: Auto



483  
 484 **Figure 4:** Box and whisker plots showing average, median, and variability (10th, 25th, 75th and 90th percentile) for  
 485 some major VOCs and the ventilation coefficients ( $\text{m}^2\text{s}^{-1}$ ) (VC) during monsoon and post-monsoon periods. The blue  
 486 and red markers represent the monsoon and post-monsoon periods, respectively.

487  
 488 Benzene which is human carcinogen is the only VOC for which there is a national ambient air quality standard (5  
 489  $\mu\text{g m}^{-3}$  equivalent to  $\sim 1.6$  ppb at 298 K) in India. Average mixing ratios in the post-monsoon season (Fig 4) were  
 490 always above this value no matter what hour of the day, and the seasonal average was twice as high as this value  
 491 ( $\sim 4$  ppb). The increased biomass burning in post-monsoon season controlled the abundance of benzene,  
 492 acetaldehyde and acetone and isoprene during this period, due to strong emissions from both biomass burning and  
 493 traffic. The typical atmospheric lifetimes of all these compounds spans from few hours (e.g. isoprene) to several  
 494 days (e.g. benzene and methanol) and several months in the case of acetonitrile. [The results of the TD-GC-FID](#)  
 495 [measurements along with the average PTR-TOF-MS values presented in Figure 4, are summarized in Figure S7.](#)  
 496 [Even though the TD-GC-FID measurements present only a snapshot as the ambient sampling duration is shorter,](#)  
 497 [the season-wise diel profiles are consistent with those obtained using the PTR-TOF-MS and the -average mixing](#)  
 498 [ratios obtained using the PTR-TOF-MS dataset also fall well within the range of mixing ratios observed using the](#)  
 499 [TD-GC-FID. This provides further confidence in the high night-time isoprene observed during the post-monsoon](#)  
 500 [season. The isoprene emissions at night during the post-monsoon season are likely due to combustion sources.](#)  
 501 [Paddy residue burning and dung burning have the highest isoprene emission factors of  \$\sim 0.2\$  g/kg \(Andreae 2019\)](#)  
 502 [and more than 8 Gg of isoprene is released in the space of a few weeks during the post-monsoon season regionally](#)  
 503 [from open paddy residue burning alone \(Kumar et al., 2021\). Previous studies from the region have also](#)  
 504 [documented isoprene emissions from non-biogenic sources, which are active also at night \(Kumar et al., 2020,](#)  
 505 [Hakkim et al., 2021\). In 2018 at another site in Delhi, using gas chromatography measurements made in pre-](#)  
 506 [monsoon and post-monsoon, Bryant et al. 2023 reported average nocturnal mixing ratios of isoprene that were 5](#)  
 507 [times higher in the post-monsoon compared to the pre-monsoon and showed different diel profiles between the](#)

508 [seasons. They found that the high night-time isoprene correlated well with carbon monoxide, a combustion tracer](#)  
509 [and suspected that in addition to the stagnant meteorological conditions, biomass burning sources could be a](#)  
510 [reason for the significant night time isoprene in Delhi in post-monsoon season and our findings using more](#)  
511 [comprehensive and high temporal resolution data further substantiate the surprising night-time isoprene.](#)

512 As potent precursors of secondary organic aerosol, the aromatic compounds would also enhance secondary  
513 organic aerosol pollutant formation during the polluted post-monsoon season. When compared with the first PTR-  
514 MS measurements of these compounds reported from wintertime Delhi (see Fig 2 of Hakkim et al., 2019), the  
515 average levels of these compounds for the post-monsoon season (Table S2) are lower or comparable, but still  
516 significantly higher than what has been reported for other major cities of the world like Tokyo, Paris, Kathmandu,  
517 Beijing, London (Yoshino et al., 2012; Dolgorouky et al., 2012; Sarkar et al., 2016; Li et al., 2019; Langford et  
518 al., 2010). The monsoon levels on the other hand were comparable to many of the other megacities.

519 As the monsoon season is characterized by favourable meteorological conditions for wet scavenging and dispersal  
520 due to higher ventilation co-efficient, as well as significantly lower open biomass burning due to wet and warm  
521 conditions, the monsoon levels can be considered as baseline values for the ambient levels of these compounds  
522 (except isoprene and acetaldehyde) in Delhi, which are driven mainly by year-round traffic and industrial sources  
523 in Delhi. In monsoon for isoprene, the major driver are biogenic sources whereas for acetaldehyde the major driver  
524 is photochemistry, a finding that is similar to what has [been](#) reported from another site in the Indo-Gangetic Plain  
525 previously (Mishra and Sinha, 2020).

#### 526 **3.4: Discovery of methanethiol (CH<sub>3</sub>SH), dichlorobenzenes (C<sub>6</sub>H<sub>4</sub>Cl<sub>2</sub>), and C6-amides (C<sub>6</sub>H<sub>13</sub>NO<sub>2</sub>) and C9- 527 organic acids (C<sub>9</sub>H<sub>18</sub>O<sub>2</sub>) in ambient Delhi air**

528 Figure 5 shows the average diel profile of four compounds present in both monsoon and post-monsoon periods  
529 that have to our knowledge never been reported from Delhi or any site in South Asia and only rarely been reported  
530 in the gas phase in any atmospheric environment in the world. Except for methanethiol detected at m/z 49.007  
531 (also called methyl mercaptan), all the other compounds namely dichlorobenzene (C<sub>6</sub>H<sub>4</sub>Cl<sub>2</sub>) detected at m/z  
532 146.977, C6-amides like hexanamide (C<sub>6</sub>H<sub>13</sub>NO<sub>2</sub>) and its isomers detected at m/z 116.108 and C9- carboxylic  
533 acid/ester such as nonanoic acid (C<sub>9</sub>H<sub>18</sub>O<sub>2</sub>) and its isomers detected at m/z 159.14, are all intermediate volatility  
534 range organic compounds. [The saturation mass concentration \(C<sub>0</sub>\) of methanethiol, C6-amide, dichlorobenzene,](#)  
535 [and C9 organic acid, were calculated using the method described in Li et al. 2016 using the following equation:](#)

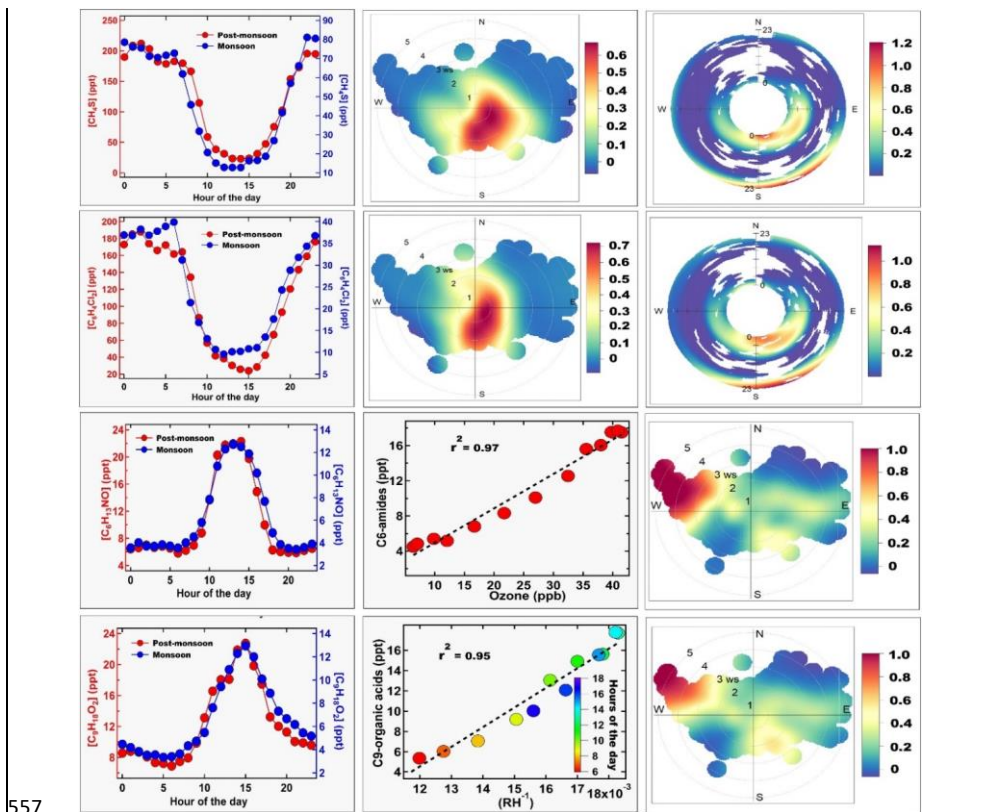
$$536 C_0 = \frac{M \cdot 10^6 \cdot p_0}{760 \cdot R \cdot T} \quad (1)$$

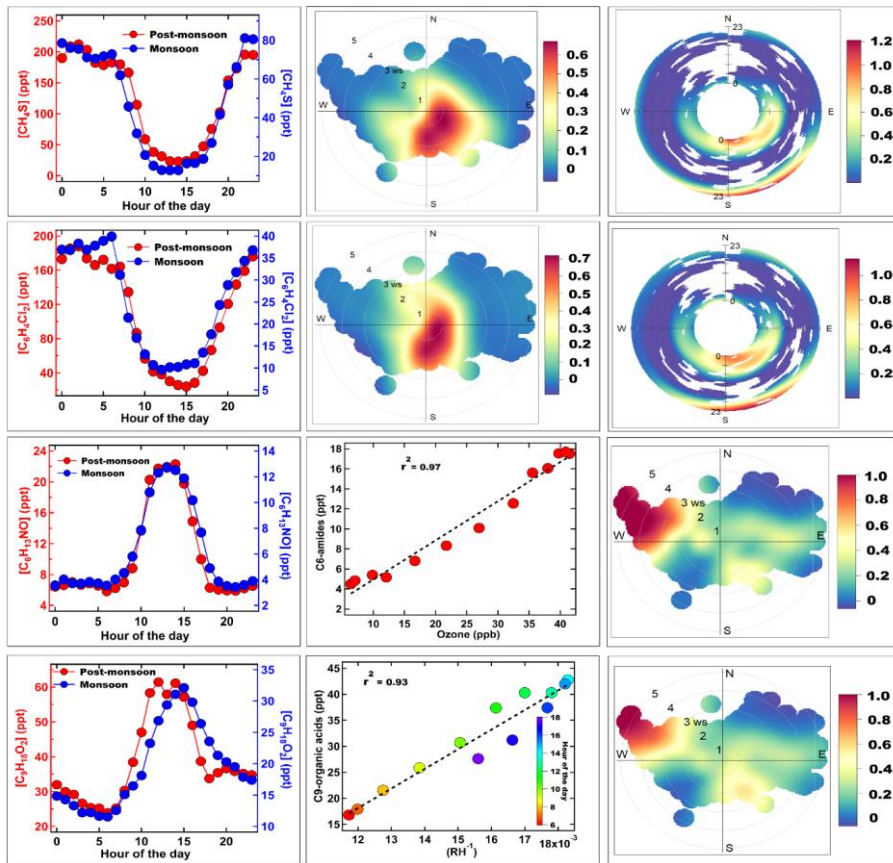
537 [wherein M is the molar mass \[g mol<sup>-1</sup>\], R is the ideal gas constant \[8.205 x 10<sup>-5</sup> atm K<sup>-1</sup> mol<sup>-1</sup> m<sup>3</sup>\], p<sub>0</sub> is the](#)  
538 [saturation vapor pressure \[mm Hg\], and T is the temperature \(K\). Organic compounds with C<sub>0</sub> > 3 x 10<sup>6</sup> µg m<sup>-3</sup>](#)  
539 [are classified as VOCs while compounds with 300 < C<sub>0</sub> < 3 x 10<sup>6</sup> µg m<sup>-3</sup> as Intermediate VOCs \(IVOCs\).](#)

540 ~~These could be detected so well, mainly due to our extended volatility range mass spectrometer design and high~~  
541 ~~sensitivity due to ion booster and hexapole guide of the PTR-TOF-MS 10-K system, which has been missing in~~  
542 ~~previous PTR-TOF-MS deployments in India.~~ The presence of such reactive organic sulphur, chlorine and  
543 nitrogen containing compounds in the gas phase [was surprising and](#) provides new insights concerning the chemical  
544 composition and secondary chemistry occurring in air, during the extremely high pollution events. Below we  
545 examine the sources and chemistry of these compounds in further detail.



546 The diel profiles of both methanethiol and dichlorobenzene in both the monsoon and post-monsoon seasons were  
 547 similar (bimodal with afternoon minima), and controlled by the ventilation coefficient diel variability (see Fig. 4),  
 548 and in fact even the difference in their average magnitudes (50 ppt Vs 130 ppt for CH<sub>3</sub>SH and 25 ppt Vs 100 ppt  
 549 for dichlorobenzene between monsoon and post-monsoon seasons), can largely be explained by the reduction in  
 550 ventilation co-efficient (~2 reduction). Further, the conditional probability wind rose plots for both compounds  
 551 shows that the high values come from the same wind sector upwind of the site spanning north-east to south during  
 552 early morning and evening hours, which is actually where a variety of industrial sources are located. Previously,  
 553 Nunes et al., (2005) and Kim et al., (2006) have reported methanethiol from petrochemical industries and landfills  
 554 in Brazil and Korea, respectively. Toda et al., (2010) reported high (tens of ppb) methanethiol mixing ratios from  
 555 a pulp and paper mill industry in Russia.  
 556





558  
 559 **Figure 5: Average diurnal profile of methanethiol, isomers of dichlorobenzene, C6-amides, and C9- organic acid in**  
 560 **the left panel for both monsoon (blue marker) and post-monsoon (red marker) periods. The second panel shows the**  
 561 **wind rose plot of methanethiol and isomers of dichlorobenzene, plot of C6-amide vs ozone and C9-organic acid vs**  
 562 **RH<sup>-1</sup> colour coded by the hour of the day. The third panel shows the polar annulus plot of methanethiol, isomers of**  
 563 **dichlorobenzene and wind rose plot of C6-amides and C9-organic acid.**

564  
 565 Both compounds are also used in the deodorant and pesticide products as reagents (Chin et al., 2013) and although  
 566 large scale pesticide manufacturing facilities were shifted out of Delhi, there are still units that sell and distribute  
 567 these products in those areas, from which fugitive emissions are likely happening. Methanethiol is further used as  
 568 a precursor in methionine production (Francois, 2023) an essential amino acid used in manufacture of pesticides,  
 569 and fragrances industry uses methanethiol for its distinct sulphur-like aroma (Bentley et al., 2004), contributing  
 570 to the creation of savory flavors and unique fragrances. In the Delhi environment, a combination of such industries,  
 571 in particular paper and pulp industries, are likely candidate sources. Figure 5 confirms that elevated methanethiol  
 572 values in the windrose had a clear directional dependence from the area spanning the north to south east sector.  
 573 This is the region where various manufacturing facilities and industrial areas of Delhi- like Patparganj (north-east)  
 574 Okhla, Faridabad (south) are situated and these industrial estates were earlier marked in Figure 1 b. Methanethiol

575 is an extremely reactive molecule reacting primarily with the hydroxyl radical (OH) during daytime with an  
576 estimated lifetime of 4.3 h (Wine et al., 1981). Its photo-oxidation in daytime with hydroxyl radicals produces  
577 sulphur dioxide, methanesulfonic acid, dimethyl disulphide and sulphuric acid (Kadota and Ishida et al., 1972;  
578 Hatakeyama et al., 1983), all of which play key roles in aerosol formation pathways. Dimethyl disulphide has a  
579 very short atmospheric lifetime spanning from 0.3 to 3 hours (Hearn et al., 1990), because of its high reactivity  
580 ( $1.98 \pm 0.18 \times 10^{-10} \text{ cm}^3 \text{ molecule}^{-1} \text{ s}^{-1}$ ) (Wine et al., 1981) with OH radicals. Although dimethydisulphide is the  
581 major product of the photo-oxidation of methanethiol (yield 50%; Wine et al., 1981), since methanethiol itself  
582 was on average only 48 ppt (monsoon) and 128 ppt (post-monsoon), and plumes occur only at night we  
583 hypothesize that the ambient concentrations of DMDS were too low to be detected by the mass spectrometer.  
584 Further it can also react with nitrate radicals (Berreshiem et al., 1995) and participate in night-time chemistry.  
585 More recently, Reed et al. (2020) performed laboratory experiments and observed that even trace amounts of  
586 organosulphur compounds, such as thiols and sulfides, can significantly enhance the organic aerosol mass  
587 concentration and its particle effective density. Though there has not been any relevant data set attributing the  
588 enhancement of organic aerosols to methanethiol in Delhi specifically, previous studies have found enhanced  
589 secondary aerosol formation rates during haze and fog episodes (Acharja et al., 2022). These studies collectively  
590 suggest an increase in the haze events in Delhi is linked to sulphur chemistry in which methanethiol due to its  
591 high reactivity and atmospheric chemistry could also be a contributor along with ammonia and other sulphur  
592 containing molecules. previous studies have found enhanced secondary aerosol formation rates during haze and  
593 fog episodes (Acharja et al., 2022). T ammonia and More recently Reed et. al. (2020) reported that presence of  
594 even trace amounts of such compounds can significantly enhance organic aerosol mass and particle effective  
595 density, and such organosulfur compounds provide evidence that sulphur and carbon chemistry coupling can  
596 impact the organic haze and atmospheric sulphur chemistry in planetary atmospheres, and to our knowledge the  
597 present study presents the first evidence from a polluted megacity supporting the hypothesis (Reed et al., 2020).  
598 Wine et al. (1981) had further predicted that the very rapid rate at which methanethiol reacts with OH would result  
599 in low steady-state concentrations in ambient air, even though reasonably large-scale sources may exist. ~~Our~~  
600 ~~findings are also consistent with this and though the ambient levels detected were few 100 ppt, the fact is that the~~  
601 ~~global methanethiol sales was 9 billion US dollars in 2023 and is expected to further grow (Coherent market~~  
602 ~~insight, last access: 19 January 2024).~~  
603 Several recent studies have reported high chloride in sub-micron aerosol of Delhi (Gani et al., 2020; Acharja et  
604 al., 2023; Pawar et al., 2023). Dichlorobenzene is an intermediate range volatile organic compound (IVOC) which  
605 can partition between gas and aerosol phase. However, till date no gaseous IVOC chlorinated organic compound  
606 have been reported in ambient air from India. p-dichlorobenzene (PDCB) also called 1, 4-dichlorobenzene, one  
607 of the dichlorobenzene isomers is known for its use as a pest repellent and deodorant in indoor environments. 1,4-  
608 dichlorobenzene in outdoor air in various locations of North America and Europe ranged from 30 ppt to 830 ppt  
609 (Chin et al., 2013). It is emitted only from anthropogenic sources as there are no known natural sources. Its  
610 emission sources include consumer and commercial products containing PDCB, waste sites, and manufacturing  
611 facilities for flavour and as insect repellent products (ATSDR. 2006). Its atmospheric lifetime is estimated to be  
612 21-45 days (Mackay et al., 1997). It has been reported as a precursor of secondary organic aerosol in indoor  
613 conditions (Komae et al., 2020). Due to its long lifetime, dichlorobenzene can be transported to upper regions of  
614 the atmosphere where some release of some reactive chlorine through photolysis can occur, but this is not likely

615 to be of large consequence. Instead, reaction with hydroxyl radicals would convert it more readily to phenolic  
616 compounds that would readily partition to aqueous aerosol phase and also undergo nitration to form nitrophenolics  
617 (Hu et al., 2021), which are a component of brown carbon (Lin et al. 2015, 2017).

618 In contrast, the diel profile of the average mixing ratios of C<sub>6</sub>H<sub>13</sub>NO (Fig. 5), likely hexanamide or isomers of C6-  
619 amides measured at m/z 116.108, was similar in both monsoon and post-monsoon season and characteristic of a  
620 compound with a purely photochemical source with no evening time peaks even during the enhanced biomass  
621 burning in post-monsoon season. As observed for several other compounds in this study, the difference in  
622 magnitude between both seasons (peak value 22 ppt in post-monsoon season vs 12 ppt in monsoon season) could  
623 be accounted for almost completely by the reduced ventilation co-efficient in post-monsoon season (factor of ~2).  
624 The presence of photochemically formed formamide and acetamide from OH oxidation of alkyl amine precursors  
625 has been previously reported (Chandra et al., 2016; Kumar et al., 2018), from another site in the Indo-Gangetic  
626 Plain which experiences strong agricultural waste burning. In the literature we could only find only one report for  
627 presence of C6 amides in the ambient air in the gas phase (Yao et al., 2016), who reported ~14 ppt in summertime  
628 air of Shanghai using an ethanol reagent ion CIMS, the source of which was both industrial and photochemical  
629 origin. However, to our knowledge this is the first study world-wide to detect and report only photo-chemically  
630 formed C6-amides in the gas phase. C6-amides are IVOCs, which can easily partition to aerosol phase depending  
631 on environmental conditions and also act as a new source of reactive organic nitrogen to the atmospheric  
632 environment. We found the highest values in air masses arriving in the afternoon from the north-west direction at  
633 high wind speeds (see Fig 5) during the post-monsoon season, which indicated that paddy stubble burning  
634 emissions of amines (Kumar et al., 2018) were its likely precursors. The mechanism of amide formation through  
635 photochemical reactions has been elucidated in several previous laboratory studies (Bunkan et al., 2016, Barnes  
636 et al., 2010; Nielsen et al., 2012; Borduas et al., 2015). When correlated with daytime ozone hourly mixing ratios,  
637 the very high correlation (r<sup>2</sup> > 0.97), confirmed its purely photochemical origin. Being an amide, further gas phase  
638 oxidation products are likely to result in organic acids or condensation on existing aerosol particles which could  
639 add to the reactive organic nitrogen in aerosol phase and neutralize acidity just like ammonia, as ammonium ion  
640 is formed from hydrolysis of amides (Yao et al., 2016). However, the exact role of these amides in nucleation and  
641 aerosol chemistry will warrant further investigations.

642 Finally, the last row of Fig. 5 shows the average mixing ratios of the compound with molecular formula C<sub>9</sub>H<sub>18</sub>O<sub>2</sub>  
643 which is likely due to isomers of C9- carboxylic acids (e.g. nonanoic acid), although one cannot rule out  
644 contributions from isomers of esters such as methyl octanoate or 2-methylbutyl isobutyrate also detected at m/z  
645 159.14. [Hartungen et al. \(2004\)](#) and more recently the insightful study by [Salvador et al. \(2022\)](#), have highlighted  
646 [that carboxylic acids \(RCOOH\) can undergo dissociation reactions within the drift tube in addition to protonation,](#)  
647 [and form acylium ions as per the following reaction below \(Hartungen et al., 2004\):](#)



650 [We detected the corresponding acylium ion of C9-carboxylic acid \(C<sub>8</sub>H<sub>17</sub>CO<sup>+</sup> detected at m/z 141.13\) in the](#)  
651 [measured ambient spectra \(Figure S9\) and found that not only was it present but that it also correlated well in the](#)  
652 [ambient data with the protonated ion \(r=0.83\). The presence of the fragment ion and its correlation, provides](#)  
653 [additional confirmation concerning the attribution of m/z 159.14 to the C9-organic acid and for quantification the](#)

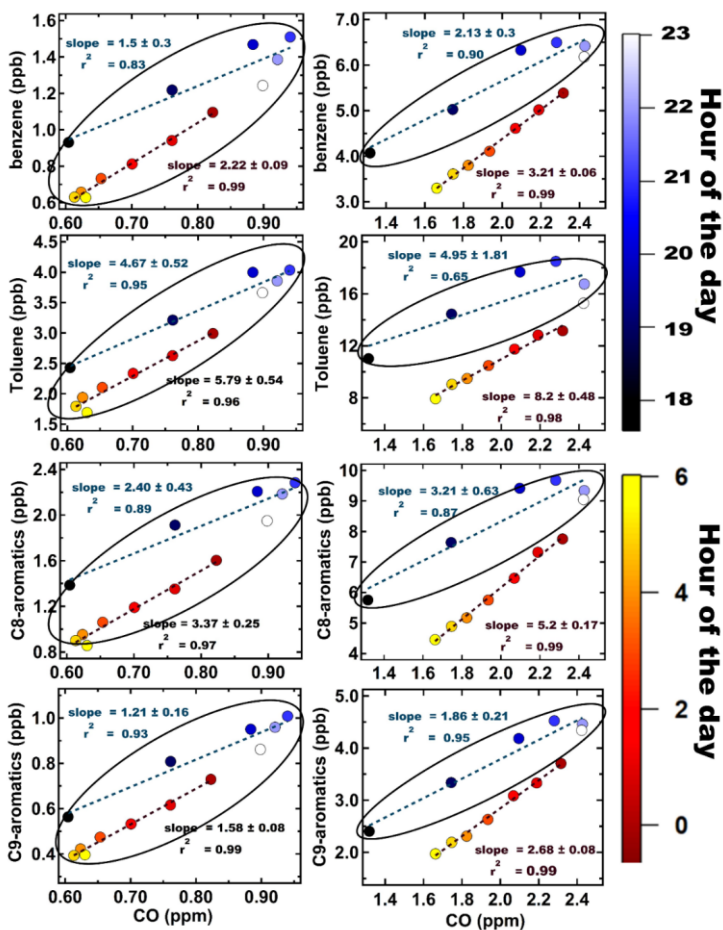
654 ion signals due to the protonated and acylium ions, were summed together for greater accuracy. Although here  
655 also there is a daytime peak, the timing of the peak is much later in the day (15:00 local time). The peak hourly  
656 values reached 6024 ppt in post-monsoon season. It showed high correlation ( $r^2 > 0.935$ ) with the inverse of the  
657 ambient daytime relative humidity indicating that it partitions back and forth between the gas phase and aerosol  
658 phase depending on the environmental conditions of temperature and RH. n-alkanoic acids in general and  
659 nonanoic acid in particular have long been reported as major organic acids present in biomass burning emitted  
660 organic aerosol (Oros et al., 2006; Fang et al., 1999). The corresponding wind rose plot (Fig. 5) shows that the  
661 highest values were in air masses arriving at high wind speeds in the afternoon from the north-west during post-  
662 monsoon season, which is a major source region of biomass burning emitted organic aerosols. It is also possible  
663 that photochemical oxidation through ozonolysis of precursors and hydroxyl radical initiated oxidation can form  
664 such carboxylic acids as an advanced oxidation product (Kawamura et al., 2013). In both cases, biomass burning  
665 emissions and evaporation from aerosol phase, appear to be the major source of this compound. Carboxylic acids  
666 in the aerosol phase would serve to neutralize some of the excess ammonia in the atmospheric environment of the  
667 Indo-Gangetic Plain (Acharja et al., 2022) and would be important for night-time aerosol chemistry in Delhi.

### 668 **3.5: Comparison of ambient mixing ratios and VOC/CO emission ratios for aromatic VOCs in Delhi with** 669 **some megacities of Asia, Europe and North America**

670 Aromatic compounds are among the most important class of compounds in urban environments due to their  
671 direct health effects (e.g. benzene is a human carcinogen), and reactivity as ozone and secondary organic aerosol  
672 precursors. Therefore, these compounds have been widely investigated in many cities and information  
673 concerning their ambient levels and emission ratios to carbon monoxide is often used for assessing similarities  
674 and differences in the sources of these compounds in varied urban environments (Warneke et al., 2007; Borbon  
675 et al., 2013). In Figure 6, we show the emission ratios (ER) derived for benzene, toluene and the sum of C8 and  
676 C9 aromatic compounds (VOC / CO ppb/ppm) using night-time monsoon (left panel) and post monsoon (right  
677 panel) measurements made in Delhi. The method is based on a linear regression fit to determine the slope of the  
678 night-time scatterplot data (from 20:00 to 06:00 L.T.) between a VOC (ppb) and CO (ppm) (de Gouw et al.,  
679 2017, Borbon et al., 2013). Using night-time hourly data (18:00 to 06:00 L.T.) provides the advantage of  
680 minimizing complications due to daytime oxidative losses of the compounds. It can be noted from Fig. 6, that  
681 during the monsoon season (from 18:00 to 23:00 and 00:00 to 06:00 local time) and post-monsoon season  
682 (18:00 to 23:00), the observed emission ratios as inferred from the slopes and fits are not statistically different  
683 from each other (all highlighted by oval circles) with values for benzene/CO, toluene/CO, sum of C8-aromatics,  
684 sum of C9-aromatics/CO in the range of 1.2-2.43, 3.14-6.76, 1.97-3.84, and 1.05-2.07, respectively. All these  
685 emission ratios fall within the range of what has been reported for typical petrol 2 and 4 wheeler vehicles in  
686 India in tail pipe emissions (Hakkim et al., 2021). For the monsoon season, although two linear fits are observed  
687 from 18:00 to 23:00 and 00:00 to 06:00, the values of the emission ratios as inferred from the respective slopes  
688 for all compounds overlap or are very close to each other and within the uncertainties for all compounds. We  
689 hypothesize that the two fits are due to the change in relative numbers of 2 wheelers and 4 wheelers. In the post-  
690 monsoon season however, for the time period in the second half of the night (00:00-06:00), the emission ratios  
691 derived from the slopes are statistically different from the ones observed in monsoon season and the first half of  
692 night in post-monsoon season (18:00-23:00). When we examined the wind rose plots for the same night-time  
693 data of the aforementioned compounds for each season (Figure S8), we noted that during the post-monsoon

Formatted: Left

694 season more pollution plumes from the south east sector which has industrial facilities and the north west sector  
695 (a major fetch region for biomass burning plumes from regional paddy residue burning in Punjab and Harvana)  
696 occurred. During the post-monsoon season due to dip in temperatures at night, the heating demand (Awasthi et  
697 al., 2024) and associated open biomass burning (Hakkim et al., 2019) also goes up, relative to the monsoon  
698 period nights. Hence overall we think that these additional sources in the post-monsoon season, do add to the  
699 burden of these mainly traffic emitted aromatic compounds and could help explain atleast partially the higher  
700 emission ratios observed during the post-monsoon season ( 00:00- 06:00), wherein values for benzene/CO,  
701 toluene/CO, sum of C8-aromatics , sum of C9-aromatics/CO values range from 3.15-3.27, 7.72-8.68, 5.03-5.37,  
702 2.6-2.76, respectively, and are statistically different from the others (ones marked by oval circles).  
703 n—second0006aforementionedIt can be noted from Fig-6, that during the monsoon season, the spread of values  
704 is much less and a single line fits the slope. For post monsoon season on the other hand, there appears to be an  
705 additional source that becomes important after the evening traffic rush hours are over and both these sources  
706 have different characteristic emission ratios (with different linear fits and slopes) with respect to CO. This  
707 suggests that in addition to traffic exhaust emissions which are a year round active source, in the post monsoon  
708 season other biomass combustion/ industrial sources also play an important role in governing the budgets of  
709 these aromatic compounds.  
710



711  
 712 **Figure 6: Emission ratios (VOC (ppb)/CO (ppm)) of benzene, toluene, C8 aromatics and C9 aromatics for both**  
 713 **monsoon (left panel) and post monsoon (right panel) periods respectively. The data points for each period are colour**  
 714 **coded with the hour of the day (18:00 L.T to 06:00 L.T).**

715  
 716 Table 1 provides a comparison of the ambient mixing ratios and emission ratios that have been reported in some  
 717 other major megacities of Asia, Europe and North America for these compounds. Although, the year of  
 718 measurements and seasons are not the same, nonetheless such comparison helps put the 2022 levels of these  
 719 compounds in Delhi in a global context. It may be further noted that we took care to calculate the emission ratios  
 720 using only night-time data when chemical loss of these compounds is negligible as their main oxidation is through  
 721 OH radicals during daytime, as also noted by de Gouw et al., 2017. Further, the other studies referred to in Table  
 722 1 for comparison, have also reported emission ratios derived using only nighttime data.

724 **Table 1: Comparative summary of the average mixing ratio (ppb) and Emission Ratios of VOC/ CO (ppb/ppm) of**  
 725 **Delhi (in parentheses) with other megacities of Asia, Europe and North America**  
 726

VOC	Delhi*	Langzhou Valley <sup>1</sup>	Sao Paulo <sup>2</sup>	London <sup>3</sup>	Los Angeles <sup>4(a)</sup>	Paris <sup>5(a)</sup>	Mexico City <sup>6(b)</sup>	New York <sup>4(c)</sup>	Beijing <sup>7(d)</sup>	Lahore <sup>8</sup>
<b>Benzene</b>	2.02 (2.65)	0.54 (1.37)	0.67 (1.03)	0.31 (1.59)	0.48 (1.30)	0.38 (1.07)	0.80 (1.21)	0.74 (1.09)	1.79 (1.24)	28.20 (5.08)
<b>Toluene</b>	5.15 (7.03)	0.72 (1.41)	2.11 (3.1)	0.60 (3.09)	1.38 (3.18)	1.40 (12.30)	3.10 (4.20)	0.19 (3.79)	1.98 (2.41)	32.40 (6.67)
<b>Sum of C8 aromatics</b>	2.74 (4.20)	0.61 (1.42)	1.52 (2.15)	0.63 (3.69)	1.03 (2.45)	1.30 (4.75)	1.10 (4.30)	0.88 (1.11)	2.66 (2.15)	29.40 (6.04)

727 \* This work (2022) <sup>1</sup>Zhou et al., (2019) <sup>2</sup>Brito et al., (2015) <sup>3</sup>Valach et al., (2014) <sup>4</sup>Baker et al., (2008)  
 728 <sup>(a)</sup>Borbon et al., (2013) <sup>5</sup>Gros et al., (2011) <sup>6</sup>Garzón et al., (2015) <sup>7</sup>Yang et al., (2019a) <sup>8</sup>Barletta et al.,  
 729 (2016) <sup>(b)</sup>Bon et al., (2011) <sup>(c)</sup>Warneke et al., (2007) <sup>(d)</sup>Wang et al., (2014) <sup>†</sup>Apel et al., (2010)  
 730

731 Except for Lahore, where benzene levels were 10 times higher, benzene levels in Delhi were comparable to Beijing  
 732 and about three times higher than those that have been reported from other megacities like Sao Paulo, London,  
 733 Los Angeles, Paris, Mexico City and New York. The annual averaged national ambient air quality standard for  
 734 benzene is 5 µg m<sup>-3</sup> in India which is approximately 1.6 ppb at room temperature. Thus, the data suggest that  
 735 sources in the investigated period (Monsoon and Post-monsoon season) would contribute to violation of the annual  
 736 averaged values. Similarly, toluene and the sum of C8 aromatic compounds (e.g. xylene and ethyl benzene  
 737 isomers) were 6 to 10 times higher in Lahore compared to Delhi and more than twice as high relative to the  
 738 aforementioned megacities, except for Beijing, where the sum of C8 aromatic compounds were comparable to  
 739 Delhi. Overall, this indicates that Delhi has much higher levels of aromatic VOC pollution than many other  
 740 megacities. When we peruse the emission ratios (ER) that have been reported for these compounds in these other  
 741 megacities (shown in parentheses in Table 1), barring few exceptions (e.g. Lahore and Paris), the ERs were  
 742 generally much higher in Delhi with an average value of 2.65, as compared to cities like Sao Paulo (Brito et al.,  
 743 2015), London (Valach et al., 2014) and Los Angeles and Paris (Borbon et al., 2013), Mexico City (Bon et al.,  
 744 2011) and several US cities (Baker et al., 2008). The ER of toluene was highest in Paris (12.3) followed by Delhi.  
 745 Overall, the mixing ratios and ERs indicate that the influence of non-traffic sources (e.g. biomass burning and  
 746 industries) is more significant in Delhi compared to many other megacities of the world. The companion paper on  
 747 source apportionment based on this dataset (Awasthi et al., 2024) will focus more on the quantitative contributions  
 748 of the different sources.

#### 749 4. Conclusion

750 This study has provided unprecedented characterization of the VOC chemical composition of ambient air in Delhi  
 751 for the clean monsoon and extremely polluted post-monsoon seasons. The total average mass concentration of the  
 752 reactive carbon in the form of the 111 VOC species identified unambiguously was ~260 µg m<sup>-3</sup> and more than 4  
 753 times higher during the polluted post-monsoon season mainly due to the impact of large scale open fires and  
 754 reduced ventilation relative to the “cleaner” monsoon season. Of the 111, 42 were pure hydrocarbons (CH), 56  
 755 were oxygenated volatile organic compounds (OVOCs; CHO), 10 were nitrogen containing compounds (NVOCs;  
 756 CHON), 2 were chlorinated volatile organic compounds (ClVOCs), and 1 namely methanethiol, contained  
 757 sulphur. The detection of new compounds that have previously not been discovered in Delhi’s air, under both the



758 clean and polluted periods such as methanethiol ( $\text{CH}_3\text{SH}$ ), dichlorobenzenes ( $\text{C}_6\text{H}_4\text{Cl}_2$ ), C6-amides ( $\text{C}_6\text{H}_{13}\text{NO}_2$ )  
759 and C9-organic acids ( $\text{C}_9\text{H}_{18}\text{O}_2$ ) in the gas phase was very surprising, considering there have been several PTR-  
760 TOF MS studies earlier (Wang et al., 2020; Tripathi et al., 2024; Jain et al., 2022). Our data pointing to both  
761 industrial sources of the sulphur and chlorine compounds, photochemical source of the C6-amides and multiphase  
762 oxidation and chemical partitioning for the C9-organic acids. To our knowledge this is the first reported study  
763 world-wide to detect and observe only photo-chemically formed C6-amides in the gas phase. C6-amides are  
764 IVOCs, which can easily partition to aerosol phase depending on environmental conditions and also act as a new  
765 source of reactive organic nitrogen to the atmospheric environment.

766 The monsoon season VOC abundances for major compounds were comparable to several other megacities of the  
767 world showing that the baseline VOC levels for the city of Delhi due to year-round active sources, helped by  
768 favourable meteorological conditions for removal of VOCs through ventilation and wet scavenging, can lead to  
769 comparable air quality as observed in other megacities. The VOC levels during the polluted post-monsoon season  
770 when severe air pollution events occur leading to shutdowns and curbs, on the other hand were significantly (2-3  
771 times) higher. ~~Overall, for many important aromatic VOCs, the levels measured in Delhi were even higher (>5~~  
772 ~~times) than many other megacities of the world located in Europe and North America. s~~ Overall, for many  
773 important aromatic VOCs, the levels measured in Delhi were even higher (> 5 times) than many other megacities  
774 of the world located in Europe and North America. Generally these aromatic compounds in megacities are  
775 primarily due to traffic and industrial emission sources, and this source is of course common to Delhi and  
776 megacities in Europe and North America. In Delhi, the highest ambient mixing ratios of these aromatic compounds  
777 occurred in the post-monsoon season. This is the period when enhanced open biomass burning occurs due to  
778 heating demand increase owing to dip in temperatures (Hakkim et al., 2019; Awasthi et al., 2024) and open fire  
779 emissions due to the seasonal post-harvest paddy stubble biomass burning in which more than 1 billion ton of  
780 biomass is burnt regionally (Kumar et al., 2021) within few weeks during mid-October to end of November occur.  
781 This adds significantly to the atmospheric burden of these compounds, compared to megacities in developed  
782 countries where open biomass burning is better and more strictly regulated. Secondly, the meteorological  
783 conditions during post-monsoon season due to shallower boundary layer height and poor ventilation, and lack of  
784 wet scavenging due to absence of rain also slow down atmospheric removal of these compounds compared to  
785 megacities in Europe, wherein it rains more frequently throughout the year compared to Delhi.

786 The presence of such a complex mixture of reactant VOCs adds to the air pollutant burden through secondary  
787 pollutant formation of aerosols. ~~The reactive gaseous organics were found to rival the high mass concentrations~~  
788 ~~of the main air pollutant in exceedance at this time, namely  $\text{PM}_{2.5}$  during the extremely polluted periods. The~~  
789 ~~reactive gaseous organics, which reached total averaged mass concentrations of  $\sim 85 \mu\text{g m}^{-3}$  (monsoon season) and~~  
790  ~~$\sim 265 \mu\text{g m}^{-3}$  (post-monsoon season) were found to rival the high mass concentrations of the main air pollutant in~~  
791 ~~exceedance at this time, namely  $\text{PM}_{2.5}$  during the extremely polluted periods (post-monsoon season average:  $\sim 145$~~   
792  ~~$\mu\text{g m}^{-3}$ - which exceeds the 24h national ambient air quality standard of  $60 \mu\text{g m}^{-3}$ ). The data of the time series of~~  
793 ~~the  $\text{PM}_{2.5}$  hourly data along with acetonitrile (a biomass burning VOC tracer) measured at the same site is provided~~  
794 ~~in Figure S10.~~ While the present study has quantified the molecules in the gas phase that are important for the air  
795 chemistry driving the high pollution events in Delhi in unprecedented detail, the implications on secondary  
796 pollutant formation will require building up on this new strategic knowledge and further investigations. Moreover,  
797 the unique primary observations will yield quantitative source apportionment of particulate matter and VOCs in

798 a companion study (Awasthi et al., 2024), that is being co-submitted to this journal to enrich the scientific  
799 insights.

800 All previous VOC studies in the literature from a dynamically growing and changing megacity like Delhi were  
801 reported for periods before 2020 (pre-COVIDeovid) times, ~~using technology that is not as state-of-the-art as~~  
802 ~~without~~ the new enhanced volatility VOC quantification technology deployed for the first time in a complex  
803 ambient environment of a developing world megacity like Delhi. These have resulted in unprecedented new  
804 information concerning the speciation, abundance, ambient variability and emission characteristics of several  
805 rarely measured/reported VOCs. The significance of the new understanding concerning atmospheric composition  
806 and chemistry of highly polluted urban atmospheric environments gained from this study, will no doubt be of  
807 global relevance as they would aid atmospheric chemistry investigations in many megacities and polluted urban  
808 environments of the global south, that are in similar development and growth trajectory as Delhi and experience  
809 extreme air pollution and air quality associated challenges, but remain understudied.

#### 810 **Data availability**

811 The primary VOC, CO and Ozone and meteorological data presented in this manuscript can be obtained  
812 downloaded by contacting Prof. Vinayak Sinha by accessing the following Mendeley doi link:  
813 <https://data.mendeley.com/preview/pb6xs2fzwc?a=7658dfde-2ca0-46c8-b89b-54ba8211e1de>

814

#### 815 **Author Contribution**

816 Sachin Mishra: Data curation, Formal analysis, Investigation, Software, Visualization, Writing – original draft  
817 preparation. Vinayak Sinha: Conceptualization, Data curation, Formal analysis, Methodology, Project  
818 administration, Software, Supervision, Validation, Writing – review & editing. Haseeb Hakkim: Data curation,  
819 Formal analysis, Investigation, Writing – review & editing. Arpit Awasthi : Data curation, Formal analysis,  
820 Investigation. Sachin D. Ghude: Writing – review & editing. Vijay Kumar Soni: Writing – review & editing. N.  
821 Nigam: resources. Baerbel Sinha: Conceptualization, Data curation, Supervision, Writing – review & editing. M.  
822 Rajeevan: Writing – review & editing.

#### 823 **Competing Interests**

824 The authors declare that they have no conflict of interest.

825

#### 826 **Acknowledgment**

827 We acknowledge the financial support given by the Ministry of Earth Sciences (MOES), Government of India, to  
828 support the RASAGAM (Realtime Ambient Source Apportionment of Gases and Aerosol for Mitigation) project  
829 at IISER Mohali vide grant MOES/16/06/2018-RDEAS Dt. 22.6.2021. S.M acknowledges IISER Mohali for  
830 Institute PhD fellowship. AA acknowledges MoE for PMRF PhD fellowship. We thank Dr. R. Mahesh, Dr. Gopal

831 Iyengar, Dr. R. Krishnan (Director, IITM Pune), Prof. Gowrishankar (Director, IISER Mohali), Dr. Mohanty (DG,  
832 IMD), Dr. M. Ravichandran (Secretary Ministry of Earth Science) for their encouragement and support. We thank  
833 student members of the Atmospheric Chemistry and Emissions (ACE) research group and Aerosol Research  
834 Group (ARG) of IISER Mohali and IITM Pune in particular Akash Vispute, Prasanna Lonkar and local scientists  
835 of IMD for their logistics and moral support. The authors gratefully acknowledge the NASA/ NOAA Suomi  
836 National Polar-orbiting Partnership (Suomi NPP) and NOAA-20 satellites VIIRS fire count data used in this  
837 publication. The authors gratefully acknowledge the NOAA Air Resources Laboratory (ARL) for the provision  
838 of the HYSPLIT transport and dispersion model used in this publication. We thank Campbell Scientific India Pvt  
839 Ltd, Ionicon Analytic GmbH and Mars Bioanalytical for technical assistance rendered by them.

#### 840 **References:**

- 841 Acharja, P., Ali, K., Ghude, S. D., Sinha, V., Sinha, B., Kulkarni, R., Gultepe, I., and Rajeevan, M. N.: Enhanced  
842 secondary aerosol formation driven by excess ammonia during fog episodes in Delhi, India, *Chemosphere* 289,  
843 133155, <https://doi.org/10.1016/j.chemosphere.2021.133155>, 2022.
- 844 Acharja, P., Ghude, S.D., Sinha, B., Barth, M., Govardhan, G., Kulkarni, R., Sinha, V., Kumar, R., Ali, K.,  
845 Gultepe, I., Petit, J., and Rajeevan, M.N., Thermodynamical framework for effective mitigation of high aerosol  
846 loading in the Indo-Gangetic Plain during winter. *Sci Rep* 13, 13667 [https://doi.org/10.1038/s41598-023-40657-](https://doi.org/10.1038/s41598-023-40657-w)  
847 [w](https://doi.org/10.1038/s41598-023-40657-w), 2023.
- 848 [Andreae, M. O.: Emission of trace gases and aerosols from biomass burning – an updated assessment, \*Atmos.\*](#)  
849 [Chem. Phys.](#), 19, 8523–8546, <https://doi.org/10.5194/acp-19-8523-2019>, 2019.
- 850 Apel, E. C., Emmons, L. K., Karl, T., Flocke, F., Hills, A. J., Madronich, S., Lee-Taylor, J., Fried, A., Weibring,  
851 P., Walega, J., Richter, D., Tie, X., Mauldin, L., Campos, T., Weinheimer, A., Knapp, D., Sive, B., Kleinman, L.,  
852 Springston, S., Zaveri, R., Ortega, J., Voss, P., Blake, D., Baker, A., Warneke, C., Welsh-Bon, D., de Gouw, J.,  
853 Zheng, J., Zhang, R., Rudolph, J., Junkermann, W., and Riemer, D. D.: Chemical evolution of volatile organic  
854 compounds in the outflow of the Mexico City Metropolitan area, *Atmos. Chem. Phys.*, 10, 2353–2375,  
855 <https://doi.org/10.5194/acp-10-2353-2010>, 2010.
- 856 ATSDR.: Toxicological Profile for 1,4-Dichlorobenzene, Atlanta, GA, Agency for Toxic Substances and Disease  
857 Registry, U.S. Department of Health and Human Services, 2006.
- 858 Awasthi, A., Sinha, B., Hakkim, H., Mishra, S., Varkrishna, M., Singh, G., Ghude, S. D., Soni, V.K., Nigam, N.,  
859 Sinha, V., and Rajeevan M.: Biomass burning sources control ambient particulate matter but traffic and industrial  
860 sources control VOCs and secondary pollutant formation during extreme pollution events in Delhi, *Atmos. Chem.*  
861 *Phys. Discuss.*, (submitted), 2024.
- 862 Baker, A. K., Beyersdorf, A. J., Doezema, L. A., Katzenstein, A., Meinardi, S., Simpson, I. J., Blake, D. R., and  
863 Sherwood Rowland, F.: Measurements of nonmethane hydrocarbons in 28 United States cities, *Atmos. Environ.*,  
864 42, 170-182, <https://doi.org/10.1016/j.atmosenv.2007.09.007>, 2008.
- 865 Barletta, B., Simpson, I. J., Blake, N. J., Meinardi, S., Emmons, L. K., Aburizaiza, O. S., Siddique, A., Zeb, J.,  
866 Yu, L. E., Khwaja, H. A., Farrukh, M. A., and Blake, D. R.: Characterization of carbon monoxide, methane and  
867 nonmethane hydrocarbons in emerging cities of Saudi Arabia and Pakistan and in Singapore, *J. Atmos. Chem.*,  
868 11, 2399–2421, <https://doi.org/10.1007/s10874-016-9343-7>, 2016.

869 Barnes, I., Solignac, G., Mellouki, A., and Becker, K. H.: Aspects of the atmospheric chemistry of  
870 amides, *ChemPhysChem*, 11(18), 3844-3857, <https://doi.org/10.1002/cphc.201000374>, 2010.

871 Bentley, R., Chasteen, T.G., Environmental VOCs—formation and degradation of dimethyl sulfide, methanethiol  
872 and related materials, *Chemosphere*, <https://doi.org/10.1016/j.chemosphere.2003.12.017> , 2004.

873 Berresheim, H., Wine, P.H., and Davis, D.D.: Sulfur in the atmosphere. In: Singh, H.B. (Ed.), *Composition,*  
874 *Chemistry, and Climate of the Atmosphere*, Van Nostrand Reinhold, New York, ISBN 0-442-01264-0, pp. 251-  
875 *307*, 1995.

876

877 Bikkina, S., Andersson, A., Kirillova, E.N., Holmstrand, H., Tiwari, S., Srivastava A. K., Bisht, D. S., and  
878 Gustafsson, O.: Air quality in megacity Delhi affected by countryside biomass burning, *Nat Sustain.*, 2, 200–205.  
879 <https://doi.org/10.1038/s41893-019-0219-0>, 2019.

880 ~~Berresheim, H., Wine, P.H., and Davis, D.D.: Sulfur in the atmosphere. In: Singh, H.B. (Ed.), *Composition,*  
881 *Chemistry, and Climate of the Atmosphere*, Van Nostrand Reinhold, New York, ISBN 0-442-01264-0, pp. 251-  
882 *307*, 1995.~~

883 Bon, D. M., Ulbrich, I. M., de Gouw, J. A., Warneke, C., Kuster, W. C., Alexander, M. L., Baker, A., Beyersdorf,  
884 A. J., Blake, D., Fall, R., Jimenez, J. L., Herndon, S. C., Huey, L. G., Knighton, W. B., Ortega, J., Springston, S.,  
885 and Vargas, O.: Measurements of volatile organic compounds at a suburban ground site (T1) in Mexico City  
886 during the MILAGRO 2006 campaign: measurement comparison, emission ratios, and source attribution, *Atmos.*  
887 *Chem. Phys.*, 11, 2399–2421, <https://doi.org/10.5194/acp-11-2399-2011>, 2011.

888 Borbon, A, Gilman, JB, Kuster, WC, Grand, N, Chevaillier, S, Colomb, A, Dolgorouky, C, Gros, V, Lopez, M,  
889 Sarda-Estevé, R, Holloway, J, Stutz, J, Petetin, H, McKeen, S, Beekmann, M, Warneke, C, Parrish, DD, and de  
890 Gouw, JA.: Emission ratios of anthropogenic volatile organic compounds in northern mid-latitude megacities:  
891 Observations versus emission inventories in Los Angeles and Paris, *J. Geophys Res.-Atmos.*, 118(4): 2041–2057.  
892 <http://dx.doi.org/10.1002/jgrd.50059>, 2013.

893 Borduas, N., da Silva, G., Murphy, J. G., and Abbatt, J. P.: Experimental and theoretical understanding of the gas  
894 phase oxidation of atmospheric amides with OH radicals: kinetics, products, and mechanisms, *J. Phys. Chem.*  
895 *A*, 119(19), 4298-4308, <https://doi.org/10.1021/jp503759f>, 2015.

896 Brito, J., Wurm, F., Yanez-Serrano, A. M., de Assuncao, J. V., Godoy, J. M., and Artaxo, P.: Vehicular Emission  
897 Ratios of VOCs in a Megacity Impacted by Extensive Ethanol Use: Results of Ambient Measurements in Sao  
898 Paulo, Brazil, *Environ. Sci. Technol.*, 49, 11381–11387, <https://doi.org/10.1021/acs.est.5b03281>, 2015.

899 Bryant, D. J., Nelson, B. S., Swift, S. J., Budisulistiorini, S. H., Drysdale, W. S., Vaughan, A. R., Newland, M. J.,  
900 Hopkins, J. R., Cash, J. M., Langford, B., Nemitz, E., Acton, W. J. F., Hewitt, C. N., Mandal, T., Gurjar, B. R.,  
901 Shivani, Gadi, R., Lee, J. D., Rickard, A. R., and Hamilton, J. F.: Biogenic and anthropogenic sources of isoprene  
902 and monoterpenes and their secondary organic aerosol in Delhi, India, *Atmos. Chem. Phys.*, 23, 61–83,  
903 <https://doi.org/10.5194/acp-23-61-2023>, 2023.

904 Bon, D. M., Ulbrich, I. M., de Gouw, J. A., Warneke, C., Kuster, W. C., Alexander, M. L., Baker, A., Beyersdorf,  
905 A. J., Blake, D., Fall, R., Jimenez, J. L., Herndon, S. C., Huey, L. G., Knighton, W. B., Ortega, J., Springston, S.,  
906 and Vargas, O.: Measurements of volatile organic compounds at a suburban ground site (T1) in Mexico City  
907 during the MILAGRO 2006 campaign: measurement comparison, emission ratios, and source attribution, *Atmos.*  
908 *Chem. Phys.*, 11, 2399–2421, <https://doi.org/10.5194/acp-11-2399-2011>, 2011.

909 [Bryant, D. J., Nelson, B. S., Swift, S. J., Budisulistiorini, S. H., Drysdale, W. S., Vaughan, A. R., Newland, M. J.,](#)  
910 [Hopkins, J. R., Cash, J. M., Langford, B., Nemitz, E., Acton, W. J. F., Hewitt, C. N., Mandal, T., Gurjar, B. R.,](#)  
911 [Shivani, Gadi, R., Lee, J. D., Rickard, A. R., and Hamilton, J. F.: Biogenic and anthropogenic sources of isoprene](#)  
912 [and monoterpenes and their secondary organic aerosol in Delhi, India, \*Atmos. Chem. Phys.\*, 23, 61–83,](#)  
913 <https://doi.org/10.5194/acp-23-61-2023>, 2023.

914 Bunkan, A. J. C., Mikoviny, T., Nielsen, C. J., Wisthaler, A., and Zhu, L. (2016): Experimental and theoretical  
915 study of the OH-initiated photo-oxidation of formamide, *J. Phys. Chem. A*, 120(8), 1222–1230,  
916 <https://doi.org/10.1021/acs.jpca.6b00032>, 2016.

917 Cash, J. M., Langford, B., Di Marco, C., Mullinger, N. J., Allan, J., Reyes-Villegas, E., Joshi, R., Heal, M. R.,  
918 Acton, W. J. F., Hewitt, C. N., Misztal, P. K., Drysdale, W., Mandal, T. K., Shivani, Gadi, R., Gurjar, B. R., and  
919 Nemitz, E.: Seasonal analysis of submicron aerosol in Old Delhi using high-resolution aerosol mass spectrometry:  
920 chemical characterisation, source apportionment and new marker identification, *Atmos. Chem. Phys.*, 21, 10133–  
921 10158, <https://doi.org/10.5194/acp-21-10133-2021>, 2021.

922 Chandra, B. P., and Sinha, V.: Contribution of post-harvest agricultural paddy residue fires in the NW Indo-  
923 Gangetic Plain to ambient carcinogenic benzenoids, toxic isocyanic acid and carbon monoxide, *Environ. Int.*, 88,  
924 187–197, <https://doi.org/10.1016/j.envint.2015.12.025>, 2016.

925 Chandra, B. P., Sinha, V., Hakkim, H., Kumar, A., Pawar, H., Mishra, A. K., Sharma, G., Pallavi, Garg, S., Ghude,  
926 S. D., Chate, D. M., Pithani, P., Kulkarni, R., Jenamani, R. K., and Rajeevan, M.: Odd–even traffic rule  
927 implementation during winter 2016 in Delhi did not reduce traffic emissions of VOCs, carbon dioxide, methane  
928 and carbon monoxide, *Curr. Sci. India* 114(6), 1318–1325, <https://www.jstor.org/stable/26797338>, 2018.

929 [Chatterji, A.: Air Pollution in Delhi: Filling the Policy Gaps, ORF Occasional Paper No. 291, December 2020,](#)  
930 [Observer Research Foundation, <https://www.orfonline.org/public/uploads/posts/pdf/20230723000625.pdf>, 2020.](#)

931 Chen, T., Zhang, P., Chu, B., Ma, Q., Ge, Y., Liu, J., and He, H.: Secondary organic aerosol formation from mixed  
932 volatile organic compounds: Effect of RO<sub>2</sub> chemistry and precursor concentration, *npj Climate and Atmospheric*  
933 *Science*, 5(1), 95. <https://doi.org/10.1038/s41612-022-00321-y>, 2022.

934 Chin, J.-Y., Godwin, C., Jia, C., Robins, T., Lewis, T., Parker, E., Max, P., and Batterman, S.: Concentrations and  
935 risks of p-dichlorobenzene in indoor and outdoor air, *Indoor Air*, 23, 40–49, [https://doi.org/10.1111/j.1600-](https://doi.org/10.1111/j.1600-0668.2012.00796.x)  
936 [0668.2012.00796.x](https://doi.org/10.1111/j.1600-0668.2012.00796.x), 2013.

937 Crippa, M., Guizzardi, D., Muntean, M., Schaaf, E., Monforti-Ferrario, F., Banja, M., Pagani, F. and Solazzo, E.:  
938 EDGAR v6.1 global air pollutant emissions, European Commission, JRC129555, 2022.

939 Coherent market insight: <https://www.coherentmarketinsights.com/market-insight/methanethiol-market-6065/>  
940 last access: 19 January 2024.

941 de Gouw, J. A., Gilman, J. B., Kim, S.-W., Lerner, B. M., IsaacmanVanWertz, G., McDonald, B. C., Warneke, C.,  
942 Kuster, W. C., Lefer, B. L., Griffith, S. M., Dusanter, S., Stevens, P. S., and Stutz, J.: Chemistry of Volatile Organic  
943 Compounds in the Los Angeles basin: Nighttime Removal of Alkenes and Determination of Emission Ratios, *J.*  
944 *Geophys. Res.-Atmos.*, 122, 11843–11861, <https://doi.org/10.1002/2017JD027459>, 2017.

945 de Gouw, J., and Warneke, C. (2007): Measurements of volatile organic compounds in the earth's atmosphere  
946 using proton-transfer-reaction mass spectrometry, *Mass spectrom. rev.*, 26(2), 223–  
947 257, <https://doi.org/10.1002/mas.20119>, 2007.

948 Dolgorouky, C., Gros, V., Sarda-Esteve, R., Sinha, V., Williams, J., Marchand, N., Sauvage, S., Poulain, L., Sciare,  
949 J., and Bonsang, B.: Total OH reactivity measurements in Paris during the 2010 MEGAPOLI winter campaign,  
950 *Atmos. Chem. Phys.*, 12, 9593–9612, <https://doi.org/10.5194/acp-12-9593-2012>, 2012.

951 Durmusoglu, E., Taspinar, F., and Karademir, A.: Health risk assessment of BTEX emissions in the landfill  
952 environment, *J. Hazard. Mater.*, 176(1-3), 870-877, <https://doi.org/10.1016/j.jhazmat.2009.11.117>, 2010.

953 Espenship, M.F., Silva, L.K., Smith, M.M., Capella, K.M., Reese, C.M., Rasio, J.P., Woodford, A.M., Geldner,  
954 N.B., Rey deCastro, B., and De Jesús, V.R.: Nitromethane exposure from tobacco smoke and diet in the US  
955 population: NHANES, 2007–2012, *Environ. Sci. Technol.* 53 (4), 2134–2140.  
956 <https://pubs.acs.org/doi/abs/10.1021/acs.est.8b05579>, 2019.

957 Fang, M., Zheng, M., Wang, F., To, K. L., Jaafar, A. B., and Tong, S. L.: The solvent-extractable organic  
958 compounds in the Indonesia biomass burning aerosols–characterization studies, *Atmos. Environ.*, 33(5), 783-795,  
959 [https://doi.org/10.1016/S1352-2310\(98\)00210-6](https://doi.org/10.1016/S1352-2310(98)00210-6), 1999.

960 François, J.M.:Progress advances in the production of bio-sourced methionine and its hydroxyl analogues.  
961 *Biotechnology Advances*, Volume 69, 108259, <https://doi.org/10.1016/j.biotechadv.2023.108259>, 2023

962 Gani, S., Bhandari, S., Patel, K., Seraj, S., Soni, P., Arub, Z., Habib, G., Hildebrandt Ruiz, L., and Apte, J.S.:  
963 Particle number concentrations and size distribution in a polluted megacity: the Delhi Aerosol Supersite study,  
964 *Atmos. Chem. Phys.* 20, 8533–8549. <https://doi.org/10.5194/acp-20-8533-2020>, 2020.

965 Garg, S., Chandra, B. P., Sinha, V., Sarda-Esteve, R., Gros, V., and Sinha, B.: Limitation of the use of the  
966 absorption angstrom exponent for source apportionment of equivalent black carbon: a case study from the North  
967 West Indo-Gangetic Plain, *Environ. Sci. Technol.* 50(2), 814-824, <https://doi.org/10.1021/acs.est.5b03868>, 2016.

968 Garzón, J. P., Huertas, J. I., Magaña, M., Huertas, M. E., Cárdenas, B., Watanabe, T., Maeda, T., Wakamatsu, S.,  
969 and Blanco, S.: Volatile organic compounds in the atmosphere of Mexico City, *Atmos. Environ.*, 119, 415–429,  
970 <https://doi.org/10.1016/j.atmosenv.2015.08.014>, 2015.

971 Graus, M., Müller, M., and Hansel, A.: High resolution PTR-TOF: quantification and formula confirmation of  
972 VOC in real time, *J. Am. Soc. Mass Spectr.*, 21(6), 1037-1044, <https://doi.org/10.1016/j.jasms.2010.02.006>, 2011.

973 Gros, V., Gaimoz, C., Herrmann, F., Custer, T., Williams, J., Bonsang, B., Sauvage, S., Locoge, N., d'Argouges,  
974 O., Sarda-Esteve, R., and Sciare, J.: Volatile organic compounds sources in Paris in spring 2007. Part I: qualitative  
975 analysis, *Environ. Chem.*, 8, 74– 90, 2011.

976 Guttikunda, S. K., Dammalapati, S. K., Pradhan, G., Krishna, B., Jethva, H. T., and Jawahar, P.: What Is Polluting  
977 Delhi's Air? A Review from 1990 to 2022, *Sustainability* 15(5), 4209; <https://doi.org/10.3390/su15054209>, 2023.

978 Hakkim, H., Kumar, A., Annadate, S., Sinha, B., and Sinha, V.: RTEII: A new high-resolution (0.1°× 0.1°) road  
979 transport emission inventory for India of 74 speciated NMVOCs, CO, NOx, NH3, CH4, CO2, PM2. 5 reveals  
980 massive overestimation of NOx and CO and missing nitromethane emissions by existing inventories, *Atmos.*  
981 *Environ.: X*, 11, 100118, <https://doi.org/10.1016/j.aeaoa.2021.100118>, 2021.

982 Hakkim, H., Sinha, V., Chandra, B. P., Kumar, A., Mishra, A. K., Sinha, B., Sharma, G., Pawar, H., Sohpaal, B.,  
983 Ghude, S.D., Pithani, P., Kulkarni, R., Jenamani, R.K., and Rajeevan, M.: Volatile organic compound  
984 measurements point to fog-induced biomass burning feedback to air quality in the megacity of Delhi, *Sci. Total*  
985 *Environ.*, 689, 295-304, <https://doi.org/10.1016/j.scitotenv.2019.06.438>, 2019.

986 Hatakeyama, S., and Akimoto, H.: Reactions of hydroxyl radicals with methanethiol, dimethyl sulfide, and  
987 dimethyl disulfide in air, *J. Phy. Chem.*, 87(13), 2387-2395, 1983.

988 Hatch, L. E., Yokelson, R. J., Stockwell, C. E., Veres, P. R., Simpson, I. J., Blake, D. R., Orlando, J. J., and  
989 Barsanti, K. C.: Multi-instrument comparison and compilation of non-methane organic gas emissions from  
990 biomass burning and implications for smoke-derived secondary organic aerosol precursors, *Atmos. Chem. Phys.*,  
991 17, 1471–1489, <https://doi.org/10.5194/acp-17-1471-2017>, 2017.

992 [Hearn, C. H., Turcu, E., and Joens, J. A.: The near U.V. absorption spectra of dimethyl sulfide, diethyl sulfide and](#)  
993 [dimethyl disulfide at T = 300 K, \*Atmos. Environ.\*, 24A, 1939–1944, 1990.](#)

994 Hersbach, H., Bell, B., Berrisford, P., Biavati, G., Horányi, A., Muñoz Sabater, J., Nicolas, J., Peubey, C., Radu,  
995 R., Rozum, I., Schepers, D., Simmons, A., Soci, C., Dee, D., and Thépaut, J.-N. (2023): ERA5 hourly data on  
996 single levels from 1940 to present. Copernicus Climate Change Service (C3S) Climate Data Store (CDS), DOI:  
997 [10.24381/cds.adbb2d47](https://doi.org/10.24381/cds.adbb2d47) (Accessed on 15-12-2023)

998 Ho, S. S. H., Yu, J. Z., Chu, K. W. and Yeung, L. L.: Carbonyl Emissions from Commercial Cooking Sources in  
999 Hong Kong, *J. Air Waste Manage. Assoc.*, 56, 1091–1098, <https://doi.org/10.1080/10473289.2006.10464532> ,  
1000 2006.

1001 Holzinger, R., Warneke, C., Hansel, A., Jordan, A., Lindinger, W., Scharffe, D. H., Schade, G., and Crutzen, P. J.:  
1002 Biomass burning as a source of formaldehyde, acetaldehyde, methanol, acetone, acetonitrile, and hydrogen  
1003 cyanide, *Geophys. Res. Lett.*, 26, 1161–1164, doi:[10.1029/1999gl900156](https://doi.org/10.1029/1999gl900156), 1999.

1004 Hu, Y., Ma, J., Zhu, M., Zhao, Y., Peng, S., and Zhu, C.: Photochemical oxidation of o-dichlorobenzene in aqueous  
1005 solution by hydroxyl radicals from nitrous acid, *J. Photoch. Photobio. A*, 420, 113503,  
1006 <https://doi.org/10.1016/j.jphotochem.2021.113503>, 2021.

1007 Li, Y., Pöschl, U., and Shiraiwa, M.: Molecular corridors and parameterizations of volatility in the chemical  
1008 evolution of organic aerosols, *Atmos. Chem. Phys.*, 16, 3327–3344, <https://doi.org/10.5194/acp-16-3327-2016> ,  
1009 2016.

1010 Jain, V., Tripathi, S.N., Tripathi, N., Sahu, L.K., Gaddamidi, S., Shukla, A.K., Bhattu, D., and Ganguly, D.:  
1011 Seasonal variability and source apportionment of non-methane VOCs using PTR-TOF-MS measurements in  
1012 Delhi, India, *Atmos. Environ.* 283, 119163, <https://doi.org/10.1016/j.atmosenv.2022.119163>, 2022.

1013 Jordan, A., Haidacher, S., Hanel, G., Hartungen, E., Märk, L., Seehauser, H., Schottkowsky, R., Sulzer, P., and  
1014 Märk, T. D.: A high resolution and high sensitivity proton-transfer-reaction time-of-flight mass spectrometer (PTR-  
1015 TOF-MS), *Int. J. Mass Spectrom.*, 286, 122–128, <https://doi.org/10.1016/j.ijms.2009.07.005>, 2009.

1016 Kadota, H., and Ishida, Y.: Production of volatile sulfur compounds by microorganisms. *Annu. Rev.*  
1017 *Microbiol.*, 26(1), 127-138, DOI: [10.1146/annurev.mi.26.100172.001015](https://doi.org/10.1146/annurev.mi.26.100172.001015), 1972.

1018 Kawamura, K., Okuzawa, K., Aggarwal, S. G., Irie, H., Kanaya, Y., and Wang, Z.: Determination of gaseous and  
1019 particulate carbonyls (glycolaldehyde, hydroxyacetone, glyoxal, methylglyoxal, nonanal and decanal) in the  
1020 atmosphere at Mt. Tai, *Atmos. Chem. Phys.*, 13, 5369–5380, <https://doi.org/10.5194/acp-13-5369-2013>, 2013.

1021 Keywood, M., Paton-Walsh, C., Lawrence, M. G., George, C., Formenti, P., Schofield, R., Cleugh, H., Borgford-  
1022 Parnell, N., and Capon, A.: Atmospheric goals for sustainable development, *Science*, 379(6629), 246-247.  
1023 doi:[10.1126/science.adg2495](https://doi.org/10.1126/science.adg2495), 2023.

1024 [Khan, I., Brimblecombe, P., and Clegg, S. L., Solubilities of Pyruvic Acid and the Lower \(C1-C6\) Carboxylic](#)  
1025 [Acids. Experimental Determination of Equilibrium Vapour Pressures Above Pure Aqueous and Salt Solutions.](#)  
1026 [Journal of Atmospheric Chemistry 22: 285-302, 1995.](#)

1027 Kim, K.: Emissions of reduced sulfur compounds (RSC) as a landfill gas (LFG): a comparative study of young  
1028 and old landfill facilities, *Atmos. Environ.* 40, 6567–6578, <https://doi.org/10.1016/j.atmosenv.2006.05.063>, 2006.

1029 Komae, S., Sekiguchi, K., Suzuki, M., Nakayama, R., Namiki, N., and Kagi, N.: Secondary organic aerosol  
1030 formation from p-dichlorobenzene under indoor environmental conditions, *Build. and Environ.* 174, 106758,  
1031 <https://doi.org/10.1016/j.buildenv.2020.106758>, 2020.

1032 Koss, A. R., Sekimoto, K., Gilman, J. B., Selimovic, V., Coggon, M. M., Zarzana, K. J., Yuan, B., Lerner, B. M.,  
1033 Brown, S. S., Jimenez, J. L., Krechmer, J., Roberts, J. M., Warneke, C., Yokelson, R. J., and de Gouw, J.: Non-  
1034 methane organic gas emissions from biomass burning: identification, quantification, and emission factors from  
1035 PTR-ToF during the FIREX 2016 laboratory experiment, *Atmos. Chem. Phys.*, 18, 3299–3319,  
1036 <https://doi.org/10.5194/acp-18-3299-2018>, 2018.

1037 Kulkarni, S.H., Ghude, S.D., Jena, C., Karumuri, R.K., Sinha, B., Sinha, V., Kumar, R., Soni, V.K., Khare, M.:  
1038 How much does large-scale crop residue burning affect the air quality in Delhi?, *Environ. Sci. Technol.* 54 (8),  
1039 4790–4799, <https://doi.org/10.1021/acs.est.0c00329>, 2020.

1040 Kumar, A., Hakkim, H., Sinha, B., and Sinha, V.: Gridded 1 km× 1 km emission inventory for paddy stubble  
1041 burning emissions over north-west India constrained by measured emission factors of 77 VOCs and district-wise  
1042 crop yield data, *Sci. Total Environ.*, 789, 148064, <https://doi.org/10.1016/j.scitotenv.2021.148064>, 2021.

1043 Kumar, A., Sinha, V., Shabin, M., Hakkim, H., Bonsang, B., and Gros, V.: Non-methane hydrocarbon (NMHC)  
1044 fingerprints of major urban and agricultural emission sources for use in source apportionment studies, *Atmos.*  
1045 *Chem. Phys.*, 20, 12133–12152, <https://doi.org/10.5194/acp-20-12133-2020>, 2020.

1046 Kumar, V., Chandra, B. P., and Sinha, V.: Large unexplained suite of chemically reactive compounds present in  
1047 ambient air due to biomass fires, *Sci. Rep.*, 8(1), 626, <https://doi.org/10.1038/s41598-017-19139-3>, 2018.

1048 Kumar, V., Sarkar, C., and Sinha, V.: Influence of post-harvest crop residue fires on surface ozone mixing ratios  
1049 in the NW IGP analyzed using 2 years of continuous in situ trace gas measurements, *J. Geophys. Res.-Atmos.*,  
1050 121(7), 3619–3633, <https://doi.org/10.1002/2015JD024308>, 2016.

1051 [Kumari, S., Verma, N., Lakhani, A., Kumari, K.M.: Severe haze events in the indo-gangetic plain during post-  
1052 monsoon: synergetic effect of synoptic meteorology and crop residue burning emission. \*Sci. Total Environ.\* 768,  
1053 145479. <https://doi.org/10.1016/j.scitotenv.2021.145479>, 2021.](https://doi.org/10.1016/j.scitotenv.2021.145479)

1054 Kurokawa, J., and Ohara, T.: Long-term historical trends in air pollutant emissions in Asia: Regional Emission  
1055 inventory in ASia (REAS) version 3, *Atmos. Chem. Phys.*, 20(21), 12761–12793, [https://doi.org/10.5194/ACP-  
1056 20-12761-2020](https://doi.org/10.5194/ACP-20-12761-2020), 2020.

1057 Langford, B., Nemitz, E., House, E., Phillips, G. J., Famulari, D., Davison, B., Hopkins, J. R., Lewis, A. C., and  
1058 Hewitt, C. N.: Fluxes and concentrations of volatile organic compounds above central London, UK, *Atmos. Chem.*  
1059 *Phys.*, 10, 627–645, <https://doi.org/10.5194/acp-10-627-2010>, 2010.

1060 Lelieveld, J., Evans, J.S., Fnais, M., Giannadaki, D., and Pozzer, A.: The contribution of outdoor air pollution  
1061 sources to premature mortality on a global scale, *Nature* 525, 367–371, <https://doi.org/10.1038/nature15371>, 2015.

1062 Li, K., Li, J., Tong, S., Wang, W., Huang, R.-J., and Ge, M.: Characteristics of wintertime VOCs in suburban and  
1063 urban Beijing: concentrations, emission ratios, and festival effects, *Atmos. Chem. Phys.*, 19, 8021–8036,  
1064 <https://doi.org/10.5194/acp-19-8021-2019>, 2019.



1065 Lin, P., Liu, J., Shilling, J. E., Kathmann, S. M., Laskin, J., and Laskin, A.: Molecular characterization of brown  
1066 carbon (BrC) chromophores in secondary organic aerosol generated from photo-oxidation of toluene,  
1067 *Phys.Chem.Chem.Phys.* 17, 23312-23325, <https://doi.org/10.1039/c5cp02563j>, 2015.

1068 Lin, P., Bluvshstein, N., Rudich, Y., Nizkorodov, S. A., Laskin, J., and Laskin, A.: Molecular Chemistry of  
1069 Atmospheric Brown Carbon Inferred from a Nationwide Biomass Burning Event, *Environ. Sci. Technol.* 51(20),  
1070 11561–11570, <https://doi.org/10.1021/acs.est.7b02276>, 2017.

1071 Mackay, D., Shiu, W. Y., and Ma, K. C.: Illustrated handbook of physical-chemical properties of environmental  
1072 fate for organic chemicals (Vol. 5). CRC press. 832pp., ISBN 978-1-56670-255-3, 1997.

1073 McDonald, B.C., de Gouw, J.A., Gilman, J.B., Jathar, S.H., Akherati, A., Cappa, C.D., Jimenez, J.L., Lee-Taylor,  
1074 J., Hayes, P.L., McKeen, S.A., Cui, Y.Y., Kim, S.W., Gentner, D.R., Isaacman-VanWertz, G., Goldstein, A.H.,  
1075 Harley, R.A., Frost, G.J., Roberts, J.M., Ryerson, T.B., and Trainer, M.: Volatile chemical products emerging as  
1076 largest petrochemical source of urban organic emissions, *Science* 359, 760e764,  
1077 <https://doi.org/10.1126/science.aag0524>, 2018.

1078 Millet, D. B., Guenther, A., Siegel, D. A., Nelson, N. B., Singh, H. B., de Gouw, J. A., Warneke, C., Williams, J.,  
1079 Eerdekens, G., Sinha, V., Karl, T., Flocke, F., Apel, E., Riemer, D. D., Palmer, P. I., and Barkley, M.: Global  
1080 atmospheric budget of acetaldehyde: 3-D model analysis and constraints from in-situ and satellite observations,  
1081 *Atmos. Chem. Phys.*, 10, 3405–3425, <https://doi.org/10.5194/acp-10-3405-2010>, 2010.

1082 Mishra, A. K., and Sinha, V.: Emission drivers and variability of ambient isoprene, formaldehyde and acetaldehyde  
1083 in north-west India during monsoon season, *Environ. Pollut.*, 267, 115538,  
1084 <https://doi.org/10.1016/j.envpol.2020.115538>, 2020.

1085 Müller, M., Mikoviny, T., Feil, S., Haidacher, S., Hanel, G., Hartungen, E., Jordan, A., Märk, L., Mutschlechner,  
1086 P., Schottkowsky, R., Sulzer, P., Crawford, J. H., and Wisthaler, A.: A compact PTR-ToF-MS instrument for  
1087 airborne measurements of volatile organic compounds at high spatiotemporal resolution, *Atmos. Meas. Tech.*, 7,  
1088 3763–3772, <https://doi.org/10.5194/amt-7-3763-2014>, 2014.

1089 Nault, B. A., Jo, D. S., McDonald, B. C., Campuzano-Jost, P., Day, D. A., Hu, W., Schroder, J. C., Allan, J., Blake,  
1090 D. R., Canagaratna, M. R., Coe, H., Coggon, M. M., DeCarlo, P. F., Diskin, G. S., Dunmore, R., Flocke, F., Fried,  
1091 A., Gilman, J. B., Gkatzelis, G., Hamilton, J. F., Hanisco, T. F., Hayes, P. L., Henze, D. K., Hodzic, A., Hopkins,  
1092 J., Hu, M., Huey, L. G., Jobson, B. T., Kuster, W. C., Lewis, A., Li, M., Liao, J., Nawaz, M. O., Pollack, I. B.,  
1093 Peischl, J., Rappenglück, B., Reeves, C. E., Richter, D., Roberts, J. M., Ryerson, T. B., Shao, M., Sommers, J. M.,  
1094 Walega, J., Warneke, C., Weibring, P., Wolfe, G. M., Young, D. E., Yuan, B., Zhang, Q., de Gouw, J. A., and  
1095 Jimenez, J. L.: Secondary organic aerosols from anthropogenic volatile organic compounds contribute  
1096 substantially to air pollution mortality, *Atmos. Chem. Phys.*, 21, 11201–11224, [https://doi.org/10.5194/acp-21-](https://doi.org/10.5194/acp-21-11201-2021)  
1097 [11201-2021](https://doi.org/10.5194/acp-21-11201-2021), 2021.

1098 Nelson, B. S., Stewart, G. J., Drysdale, W. S., Newland, M. J., Vaughan, A. R., Dunmore, R. E., Edwards, P. M.,  
1099 Lewis, A. C., Hamilton, J. F., Acton, W. J., Hewitt, C. N., Crilley, L. R., Alam, M. S., Şahin, Ü. A., Beddows, D.  
1100 C. S., Bloss, W. J., Slater, E., Whalley, L. K., Heard, D. E., Cash, J. M., Langford, B., Nemitz, E., Sommariva, R.,  
1101 Cox, S., Shivani, Gadi, R., Gurjar, B. R., Hopkins, J. R., Rickard, A. R., and Lee, J. D.: In situ ozone production  
1102 is highly sensitive to volatile organic compounds in Delhi, India, *Atmos. Chem. Phys.*, 21, 13609–13630,  
1103 <https://doi.org/10.5194/acp-21-13609-2021>, 2021.

1104 Nielsen, C. J., Herrmann, H., and Weller, C.: Atmospheric chemistry and environmental impact of the use of  
1105 amines in carbon capture and storage (CCS), *Chemical Society Reviews*, 41(19), 6684-6704,  
1106 <https://doi.org/10.1039/C2CS35059A>, 2012.

1107 Nunes, L.S., Tavares, T.M., Dippel, J., and Jaeschke, W.: Measurements of Atmospheric Concentrations of  
1108 Reduced Sulphur Compounds in the All Saints Bay Area in Bahia, Brazil, *J. Atmos. Chem.*, 50, 79-100,  
1109 <https://doi.org/10.1007/s10874-005-3123-0>, 2005.

1110 Oros, D. R., bin Abas, M. R., Omar, N. Y. M., Rahman, N. A., and Simoneit, B. R.: Identification and emission  
1111 factors of molecular tracers in organic aerosols from biomass burning: Part 3. Grasses, *Appl. Geochem.* 21(6),  
1112 919-940, <https://doi.org/10.1016/j.apgeochem.2006.01.008>, 2006.

1113 Pagonis, D., Sekimoto, K., and de Gouw, J.: A library of proton-transfer reactions of H<sub>3</sub>O<sup>+</sup> ions used for trace gas  
1114 detection, *J. Am. Soc. Mass Spectr.*, 30(7), 1330-1335, <https://doi.org/10.1007/s13361-019-02209-3>, 2019.

1115 Pawar, H., Garg, S., Kumar, V., Sachan, H., Arya, R., Sarkar, C., Chandra, B. P., and Sinha, B.: Quantifying the  
1116 contribution of long-range transport to particulate matter (PM) mass loadings at a suburban site in the north-  
1117 western Indo-Gangetic Plain (NW-IGP), *Atmos. Chem. Phys.*, 15, 9501–9520, [https://doi.org/10.5194/acp-15-](https://doi.org/10.5194/acp-15-9501-2015)  
1118 [9501-2015](https://doi.org/10.5194/acp-15-9501-2015), 2015.

1119 Pawar, P. V., Ghude, S. D., Govardhan, G., Acharja, P., Kulkarni, R., Kumar, R., Sinha, B., Sinha, V., Jena, C.,  
1120 Gunwani, P., Adhya, T. K., Nemitz, E., and Sutton, M. A.: Chloride (HCl/Cl<sup>-</sup>) dominates inorganic aerosol  
1121 formation from ammonia in the Indo-Gangetic Plain during winter: modeling and comparison with observations,  
1122 *Atmos. Chem. Phys.*, 23, 41–59, <https://doi.org/10.5194/acp-23-41-2023>, 2023.

1123 Piel, F., Müller, M., Winkler, K., Skytte af Sättra, J., and Wisthaler, A.: Introducing the extended volatility range  
1124 proton-transfer-reaction mass spectrometer (EVR PTR-MS), *Atmos. Meas. Tech.*, 14, 1355–1363,  
1125 <https://doi.org/10.5194/amt-14-1355-2021>, 2021.

1126 Reed, N. W., Browne, E. C., and Tolbert, M. A.: Impact of hydrogen sulfide on photochemical haze formation in  
1127 methane/nitrogen atmospheres, *ACS Earth and Space Chemistry*, 4(6), 897-904,  
1128 <https://doi.org/10.1021/acsearthspacechem.0c00086>, 2020.

1129 [Reinecke, T., Leiminger, M., Klinger, A., and Müller, M.: Direct detection of polycyclic aromatic hydrocarbons](https://doi.org/10.5194/ar-2-225-2024)  
1130 [on a molecular composition level in summertime ambient aerosol via proton transfer reaction mass spectrometry,](https://doi.org/10.5194/ar-2-225-2024)  
1131 [Aerosol Research](https://doi.org/10.5194/ar-2-225-2024), 2, 225–233, <https://doi.org/10.5194/ar-2-225-2024>, 2024.

1132 Roberts, J. M., Veres, P. R., Cochran, A. K., Warneke, C., Burling, I. R., Yokelson, R. J., Lerner, B., Gilman, J. B.,  
1133 Kuster, W. C., Fall, R., and de Gouw, J.: Isocyanic acid in the atmosphere and its possible link to smoke-related  
1134 health effects, *Proc. Natl. Acad. Sci. USA*, 108, 8966–8971, <https://doi.org/10.1073/pnas.1103352108>, 2011.

1135 Salvador, C. M., Chou, C. C. K., Ho, T. T., Ku, I. T., Tsai, C. Y., Tsao, T. M., Tsai, M. J., and Su, T. C.: Extensive  
1136 urban air pollution footprint evidenced by submicron organic aerosols molecular composition, *npj Climate and*  
1137 *Atmospheric Science*, 5, 96, <https://doi.org/10.1038/s41612-022-00314-x>, 2022.

1138 Sarkar, C., Sinha, V., Kumar, V., Rupakheti, M., Panday, A., Mahata, K. S., Rupakheti, D., Kathayat, B., and  
1139 Lawrence, M. G.: Overview of VOC emissions and chemistry from PTR-TOF-MS measurements during the  
1140 SusKat-ABC campaign: high acetaldehyde, isoprene and isocyanic acid in wintertime air of the Kathmandu  
1141 Valley, *Atmos. Chem. Phys.*, 16, 3979–4003, <https://doi.org/10.5194/acp-16-3979-2016>, 2016.

1142 [Shabin, M., Khatarkar, P., Hakkim, H., et al., Monsoon and post-monsoon measurements of 53 non-methane](#)  
1143 [hydrocarbons \(NMHCs\) in megacity Delhi and Mohali reveal similar NMHC composition across seasons, \*Urban\*](#)  
1144 [Climate, Volume 55, 101983, 2024.](#)

1145 Sharma, S. K., and Mandal, T. K.: Elemental composition and sources of fine particulate matter (PM<sub>2.5</sub>) in Delhi,  
1146 India, *Bulletin of Environmental Contamination and Toxicology*, 110(3), 60. [https://doi.org/10.1007/s00128-023-](https://doi.org/10.1007/s00128-023-03707-7)  
1147 [03707-7](https://doi.org/10.1007/s00128-023-03707-7), 2023.

1148 Singh, D. P., Gadi, R., and Mandal, T. K.: Characterization of particulate-bound polycyclic aromatic hydrocarbons  
1149 and trace metals composition of urban air in Delhi, India, *Atmos. Environ.*, 45(40), 7653-7663,  
1150 <https://doi.org/10.1016/j.atmosenv.2011.02.058>, 2011.

1151 Singh, R., Sinha, B., Hakkim, H., and Sinha, V.: Source apportionment of volatile organic compounds during  
1152 paddy-residue burning season in north-west India reveals large pool of photochemically formed air  
1153 toxics, *Environ. Pollut.*, 338, 122656, <https://doi.org/10.1016/j.envpol.2023.122656>, 2023.

1154 Sinha, V., Kumar, V., and Sarkar, C.: Chemical composition of pre-monsoon air in the Indo-Gangetic Plain  
1155 measured using a new air quality facility and PTR-MS: high surface ozone and strong influence of biomass  
1156 burning, *Atmos. Chem. Phys.*, 14, 5921–5941, <https://doi.org/10.5194/acp-14-5921-2014>, 2014.

1157 Stark, H., Yataavelli, R. L. N., Thompson, S. L., Kimmel, J. R., Cubison, M. J., Chhabra, P. S., Canagaratna, M.  
1158 R., Jayne, J. T., Worsnop, D. R., and Jimenez, J. L.: Methods to extract molecular and bulk chemical information  
1159 from series of complex mass spectra with limited mass resolution, *Int. J. Mass Spectrom.*, 389, 26–38,  
1160 <https://doi.org/10.1016/j.ijms.2015.08.011>, 2015.

1161 Stockwell, C. E., Veres, P. R., Williams, J., and Yokelson, R. J.: Characterization of biomass burning emissions  
1162 from cooking fires, peat, crop residue, and other fuels with high-resolution proton-transfer-reaction time-of-flight  
1163 mass spectrometry, *Atmos. Chem. Phys.*, 15, 845–865, <https://doi.org/10.5194/acp-15-845-2015>, 2015.

1164 Toda, K., Obata, T., Obokin, V. A., Potemkin, V. L., Hirota, K., Takeuchi, M., Arita, S., Khodzher, T. V., and  
1165 Grachev, M. A.: Atmospheric methanethiol emitted from a pulp and paper plant on the shore of Lake Baikal,  
1166 *Atmos. Environ.*, 44, 2427–2433, doi:[10.1016/j.atmosenv.2010.03.037](https://doi.org/10.1016/j.atmosenv.2010.03.037), 2010.

1167 Tripathi, N., Sahu, L. K., Wang, L., Vats, P., Soni, M., Kumar, P., Satish, R. V., Bhattu, D., Sahu, R., Patel, K.,  
1168 Rai, P., Kumar, V., Rastogi, N., Ojha, N., Tiwari, S., Ganguly, D., Slowik, J., Prévôt, A. S. H., and Tripathi, S. N.:  
1169 Characteristics of VOC Composition at Urban and Suburban Sites of New Delhi, India in Winter, *J. Geophys.*  
1170 *Res.-Atmos.*, 127, e2021JD035342, <https://doi.org/10.1029/2021JD035342>, 2022.

1171 Valach, A. C., Langford, B., Nemitz, E., MacKenzie, A. R., and Hewitt, C. N.: Concentrations of selected volatile  
1172 organic compounds at kerbside and background sites in central London, *Atmos. Environ.*, 95, 456–467,  
1173 <https://doi.org/10.1016/j.atmosenv.2014.06.052>, 2014.

1174 Wang, M., Shao, M., Chen, W., Yuan, B., Lu, S., Zhang, Q., Zeng, L., and Wang, Q.: A temporally and spatially  
1175 resolved validation of emission inventories by measurements of ambient volatile organic compounds in Beijing,  
1176 China, *Atmos. Chem. Phys.*, 14, 5871–5891, <https://doi.org/10.5194/acp-14-5871-2014>, 2014.

1177 Wang, L., Slowik, J. G., Tripathi, N., Bhattu, D., Rai, P., Kumar, V., Vats, P., Satish, R., Baltensperger, U., Ganguly,  
1178 D., Rastogi, N., Sahu, L. K., Tripathi, S. N., and Prévôt, A. S. H.: Source characterization of volatile organic  
1179 compounds measured by proton-transfer-reaction time-of-flight mass spectrometers in Delhi, India, *Atmos. Chem.*  
1180 *Phys.*, 20, 9753–9770, <https://doi.org/10.5194/acp-20-9753-2020>, 2020.

1181 Warneke, C., Holzinger, R., Hansel, A., Jordan, A., Lindinger, W., Poschl, U., Williams, J., Hoor, P., Fischer, H.,  
1182 Crutzen, P.J., Scheeren, H.A., and Lelieveld, J.: Isoprene and its oxidation products methyl vinyl ketone,  
1183 methacrolein, and isoprene related peroxides measured online over the tropical rain forest of Surinam in March  
1184 1998, *J. Atmos. Chem.*, 38, 167–185, <https://doi.org/10.1023/A:1006326802432>, 2001.

1185 Warneke, C., McKeen, S. A., de Gouw, J. A., Goldan, P. D., Kuster, W. C., Holloway, J. S., Williams, E. J., Lerner,  
1186 B. M., Parrish, D. D., Trainer, M., Fehsenfeld, F. C., Kato, S., Atlas, E. L., Baker, A., and Blake, D. R.:  
1187 Determination of urban volatile organic compound emission ratios and comparison with an emissions database,  
1188 *J. Geophys. Res.*, 112, D10S47, <https://doi.org/10.1029/2006JD007930>, 2007.

1189 Weng, M., Zhu, L., Yang, K., and Chen, S.: Levels and health risks of carbonyl compounds in selected public  
1190 places in Hangzhou, China, *J. Hazard. Mater.*, 164(2-3), 700-706, <https://doi.org/10.1016/j.jhazmat.2008.08.094>,  
1191 2009.

1192 WHO Guidelines for Indoor Air Quality: Selected Pollutants, edited by: Theakston, F., World Health Organization:  
1193 WHO Regional Office for Europe, Copenhagen, Denmark, 1–454, 2010.

1194 WHO 2019.: Exposure to benzene: a major public health concern: [https://www.who.int/publications/i/item/WHO-](https://www.who.int/publications/i/item/WHO-CED-PHE-EPE-19.4.2)  
1195 [CED-PHE-EPE-19.4.2](https://www.who.int/publications/i/item/WHO-CED-PHE-EPE-19.4.2), last access: 19 January 2024.

1196 Wine, P. H., Kreutter, N. M., Gump, C. A., and Ravishankara, A. R.: Kinetics of hydroxyl radical reactions with  
1197 the atmospheric sulfur compounds hydrogen sulfide, methanethiol, ethanethiol, and dimethyl disulfide, *J. Phys.*  
1198 *Chem.*, 85(18), 2660-2665, 1981.

1199 Yáñez-Serrano, A. M., Filella, I., LLusià, J., Gargallo-Garriga, A., Granda, V., Bourtsoukidis, E., Williams, J.,  
1200 Seco, R., Cappellin, L., Werner, C., de Gouw, J., and Peñuelas, J.: GLOVOCS - Master compound assignment  
1201 guide for proton transfer reaction mass spectrometry users, *Atmos. Environ.* 244, 117929,  
1202 <https://doi.org/10.1016/J.ATMOSENV.2020.117929>, 2021.

1203 Yao, L., Wang, M.-Y., Wang, X.-K., Liu, Y.-J., Chen, H.-F., Zheng, J., Nie, W., Ding, A.-J., Geng, F.-H., Wang,  
1204 D.-F., Chen, J.-M., Worsnop, D. R., and Wang, L.: Detection of atmospheric gaseous amines and amides by a  
1205 high-resolution time-of-flight chemical ionization mass spectrometer with protonated ethanol reagent ions, *Atmos.*  
1206 *Chem. Phys.*, 16, 14527–14543, <https://doi.org/10.5194/acp-16-14527-2016>, 2016.

1207 Yoshino, A., Nakashima, Y., Miyazaki, K., Kato, S., Suthawaree, J., Shimo, N., Matsunaga, S., Chatani, S., Apel,  
1208 E., Greenberg, J., Guenther, A., Ueno, H., Sasaki, H., Hoshi, J. Y., Yokota, H., Ishii, K., and Kajii, Y.: Air quality  
1209 diagnosis from comprehensive observations of total OH reactivity and reactive trace species in urban central  
1210 Tokyo, *Atmos. Environ.*, 49, 51–59, doi:10.1016/j.atmosenv.2011.12.029, 2012.

1211 Yuan, B., Koss, A.R., Warneke, C., Coggon, M., Sekimoto, K., and de Gouw, J.: Proton-Transfer Reaction Mass  
1212 Spectrometry: Applications in Atmospheric Sciences, *Chem. Rev.* 117 (21), 13187-13229,  
1213 <https://doi.org/10.1021/acs.chemrev.7b00325>, 2017.

1214 Zhou, X., Li, Z., Zhang, T., Wang, F., Wang, F., Tao, Y., Zhang, X., Wang, F., and Huang, J.: Volatile organic  
1215 compounds in a typical petrochemical industrialized valley city of northwest China based on high-resolution PTR-  
1216 MS measurements: Characterization, sources and chemical effects, *Sci. Total Environ.*, 671, 883– 896,  
1217 <https://doi.org/10.1016/j.scitotenv.2019.03.283>, 2019.

1218